EFFECT OF ADDITION OF CNTs

ON

PROPERTIES OF CONCRETE

A Dissertation submitted
In partial Fulfilment of the Requirements for
the award of degree of

MASTERS OF ENGINEERING

IN

CIVIL (STRUCTURES)

ENGINEERING

Submitted by

GURPREET SINGH SETHI
(ROLL NO. 801222005)

Under the guidance of

Dr. PREM PAL BANSAL
Assistant Professor

CIVIL ENGINEERING DEPARTMENT

THAPAR UNIVERSITY, PATIALA- 147004

JULY 2014

CERTIFICATE

Certified that the thesis **"EFFECT OF ADDITION OF CNTs ON PROPERTIES OF CONCRETE"** which is submitted by **Mr Gurpreet Singh Sethi**, in fulfilment of the requirement for the award of the degree of Master of Technology in the **Department of Civil Engineering (CED)**, Thapar University, Patiala, is a record of the candidate's own independent and original research work carried out under supervision and guidance of **Dr. Prem Pal Bansal**. The matter embodied in this thesis has not been submitted in part or full to any other University or Institute for the award of any degree.

Gurpreet Singh

Date: **Gurpreet Singh Sethi**

It is certified that the above statement made by the student concerned is correct to best of my knowledge and belief.

(Dr. Prem Pal Bansal)
Guide, Assistant Professor
CED, Thapar University
Patiala-147004

Countersigned by:

(Dr. Naveen Kwatra)
Head, CED
Thapar University,
Patiala-147004

(Dr.S.K. Mohapatra)
Dean, AcademicsAffairs,
Thapar University,
Patiala-147004

i

ACKNOWLEDGEMENT

I express my deep gratitude and respects to my supervisor **Dr. Prem Pal Bansal, Assistant Professor in Civil Engineering Department,** for their keen interest and valuable guidance, stron motivation and constant encouragement during the course of work. I thank him for their great patience, constructive criticism and myriad useful suggestions apart from in valuable guidance to me. My first and foremost offering of thanks goes to the architect who shaped my dreams into reality.

I would like to convey my sincere gratitude to my friends and colleagues for their support, co-operation and their timely help and valuable discussions.

I owe my sincere thanks to all the staff members of **Civil Engineering Department** for their support and encouragement. The meaning of my life and work is incomplete without paying regards to my respected parents whose blessings and continuous encouragement have shown me the path to achieve the goals.

And above all, I pay my regards to the **Almighty** for his love and blessings.

Gurpreet Singh Sethi

ME Civil (Structures)

Regd. No. 801222005

ABSTRACT

Carbon nanotubes (CNTs) are now known to be the materials of 21st century and are currently receiving a lot of interests due to its extremely good mechanical properties. CNTs resemble single or multiple graphene sheets rolled up in a tube or a series of tubes. The unique graphene structure endows CNTs with extraordinary characteristics. While their density is less than that of steel or glass fiber, CNTs have an elastic modulus in the terapascal range, yield strength of approximately 20-60GPa, and yield strain of up to 10 percent. CNTs have high aspect ratios and strong van der Waals self-attraction between nanotubes and tend to form CNT bundles. When CNTs are used in concrete, they were expected to provide mechanical reinforcement between hydration products of cement with nano-scale dimensions. CNTs/CNFs achieves enhancement effect by nucleation, increasing the amount of C-S-H gel of high hardness, improving pore structures, controlling nanoscale cracks, improving the early strain capacity and reducing autogenous shrinkage etc. These mechanisms would also improve the durability of cement-based materials.

In the present study, the effect of addition of CNTs on strength and durabilty properties of concrete has been studied. Five different mixes were prepared, in which fly ash was utilized in replacement with cement (20%) by weight and CNTs in different percentages (0.025%, 0.048%, and 0.08%) to (cement + fly ash) by weight. The evaluated strength properties (compressive strength, splitting tensile strength and young's modulus) and durability property (permeability) were compared with the sample containing 20 percent fly ash only and with each other on different utilized percentages of CNTs. Increase in compressive strength, splitting tensile strength and young's modulus was observed in the mix incorporating 0.08% CNTs and FA on comparison with mixture containing 20 percent fly ash. Also the mix incorporating 0.08% CNTs and FA exhibited low permeability to chloride ions and hence enhancing the durability properties of concrete mix.

CONTENTS

LIST OF FIGURES

LIST OF TABLES

CHAPTER 1

INTRODUCTION

1.1 GENERAL

Concrete construction is likely to give trouble free service throughout in the design life. However, these opportunities are not realised in many constructions because of structural deficiency, material weakening, unexpected over loadings or physical damage. Premature material weakening arises from number of causes, the most common being when the constructional specifications are violated or due to the exposure to the harsher service environment than those anticipated during the planning and design stages. Physical damages can also arise from fire explosions etc. Except in extreme cases, most of the structures require renovation to meet its functional requirements by considering appropriate repair techniques.

In the present world, various types of measures are employed to repair the concrete structures rather to build them again. These measures are retrofitting; FRP's, etc. Also along with these measures, nanotechnology plays a quite important role in the field of researches. Various nanomaterials are fullerenes, quantum dots, nanowires, nonorods, nanosilica. These are used as an additive in concrete and improve the mechanical and durability properties of concrete. Fly ash being employed in concrete from the past times also has a vital role in improving the strength properties of concrete. In the earlier ages, fly ash has not much influence on strength because strength goes on decreasing but at later ages, properties tend to increase. Hence this is also utilized in concrete structures where strength at earlier ages is not an issue.

1.2 NANOMATERIALS

Nanomaterials are defined as materials with at least one external dimension in the size range from approximately 1-100 nanometres. Nanoparticles that are naturally occurring (e.g., volcanic ash, soot from forest fires) or are the incidental by-products of combustion processes (e.g., welding, diesel engines) are usually physically and chemically heterogeneous and often termed ultrafine particles. Engineered nanoparticles are deliberately produced and designed with very definite properties related to shape, size, surface properties and chemistry. These properties are reflected in aerosols, colloids, or powders. Often, the behaviour of nanomaterials may depend more on surface area than particle composition itself. Relative surface area is one of the principal factors that enhance its reactivity, strength and electrical properties.

Engineered nanoparticles may be bought from commercial vendors or generated via experimental procedures by researchers in the laboratory (e.g., CNTs can be produced by laser ablation, HiPCO (high-pressure carbon monoxide, arc discharge, and chemical vapor deposition (CVD)). Examples of engineered nanomaterials include: carbon buckeyballs or fullerenes; carbon nanotubes; metal or metal oxide nanoparticles (e.g., gold, titanium dioxide); quantum dots, nano silica, titanium dioxide, nano clay, cerium dioxide, etc.

1.3 CARBON NANOTUBES

Carbon nanotubes (CNTs) are allotropes of carbon with a cylindrical nanostructure. Nanotubes have been constructed with length-to-diameter ratio of up to 132,000,000:1, significantly larger than for any other material. These cylindrical carbon molecules have unusual properties, which are valuable for nanotechnology, electronics, optics and other fields of materials science and technology. In addition to their thermal conductivity, mechanical and electrical properties, carbon nanotubes are also found useful in other fields like as they can be used as additives to various structural materials. For instance, nanotubes form a tiny portion of the material(s) in some (primarily carbon fibre) baseball bats, golf clubs, or car parts.

Nanotubes are members of the fullerene structural family. Their name is derived from their long, hollow structure with the walls formed by one-atom-thick sheets of carbon, called graphene. These sheets are rolled at specific and discrete ("chiral") angles, and the combination of the rolling angle and radius decides the nanotube properties; for example, whether the individual nanotube shell is a metal or semiconductor. Nanotubes are categorized as single-walled nanotubes (SWNTs) and multi-walled nanotubes (MWNTs). Individual nanotubes naturally align themselves into "ropes" held together by van der Waals forces, more specifically, pi-stacking. Applied quantum chemistry, specifically, orbital hybridization best describes chemical bonding in nanotubes. The chemical bonding of nanotubes is composed entirely of sp^2 bonds, similar to those of graphite. These bonds, which are stronger than the sp^3 bonds found in alkanes and diamond, provide nanotubes with their unique strength.

1.4 HISTORY OF CARBON NANOTUBES

Carbon nanotubes with nanoscale dimension (1-D) have been well-known over the past 15 years. In the 1950s, there was an initial discovery of first carbon nanotubes by

Roger Bacon. He was credited with the first visual impression of the tubes of atoms that roll up and are capped with fullerene molecules by many scientists in the field.

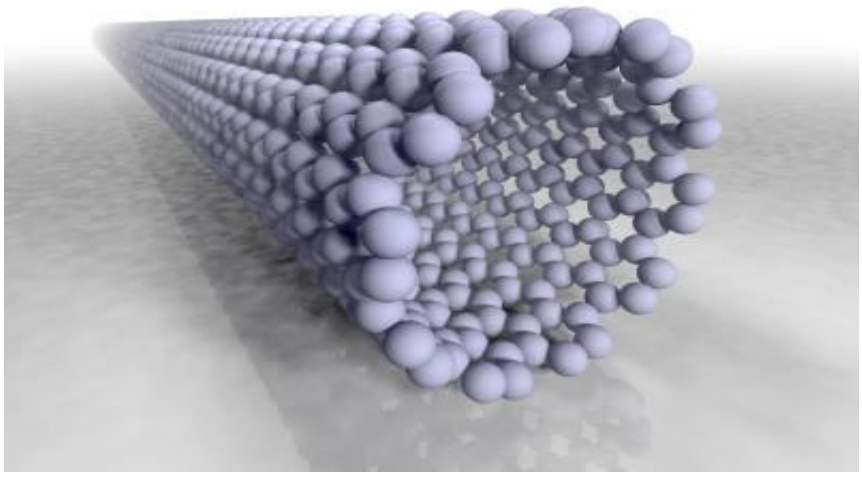

Fig. 1.1 First observation of Carbon nanotubes by Roger bacon

But at this early stage, nobody believed that whether his discovery could impact scientific research or not.

In 1952 L. V. Radushkevich and V. M. Lukyanovich published clear images of 50 nm diameter tubes made of carbon in the Soviet Journal of Physical Chemistry, but the main problem arises that the article was published in Russian language. It was likely that carbon nanotubes were produced before this date, but the discovery of the transmission electron microscope (TEM) allowed direct visualization of these structures.

Oberlin, Endo and Koyama published a paper in 1976 clearly showed hollow carbon fibers with nanometer-scale diameters by the use of vapour-growth technique. Additionally, the authors showed a TEM image of a nanotube consisting of a single wall of graphene. Later, Endo has referred to this image as a single-walled nanotube.

In 1979, John Abrahamson showed evidence of carbon nanotubes at the 14th Biennial Conference of Carbon at Pennsylvania State University. The conference paper described carbon nanotubes as carbon fibers that were produced on carbon anodes during arc discharge. A characterization of these fibers was given as well as hypotheses for their growth in a nitrogen atmosphere at low pressures.

In 1981, a group of Soviet scientists published the results of chemical and structural characterization of carbon nanoparticles produced by a thermocatalytical

disproportionation of carbon monoxide. Using TEM images and XRD patterns, the authors suggested that their “carbon multi-layer tubular crystals” were formed by rolling graphene layers into cylinders. They speculated that by rolling graphene layers into a cylinder, many different arrangements of graphene hexagonal nets were possible. They suggested two possibilities of such arrangements: circular arrangement (armchair nanotube) and a spiral, helical arrangement (chiral tube).

In 1987, Howard G. Tennett of Hyperion Catalysis was issued a U.S. patent for the production of “cylindrical discrete carbon fibrils” with a “constant diameter between about 3.5 and about 70 nanometers, length 10^2 times the diameter, and an outer region of multiple essentially continuous layers of ordered carbon atoms and a distinct inner core’’

In 1991, Iijima's discovered multi-walled carbon nanotubes in the insoluble material of arc-burned graphite rods. On the other hand, Mintmire, Dunlap, White's predicted that if single-walled carbon nanotubes could be made, then they would demonstrate remarkable conducting properties.

In 1991, Iijima during his study on the synthesis of fullerenes by using electric arc discharge technique discovered multi-walled carbon nanotubes (MWNTs), like as Russian dolls, containing at least two graphene layers, and generally have inner diameters of approximately 4 nm. Two years later, Iijima and Ichihashi of NEC and Bethune and colleagues of the IBM Almaden Research Center in California synthesized single-walled carbon nanotubes (SWNTs). The SWNTs were synthesized by the same procedure of producing MWNTs but by adding transition-metal catalysts to the carbon. The arc discharge technique was well-known to produce the famed Buckminster fullerene on a preparative scale, and these results appeared to extend the run of accidental discoveries relating to fullerenes. The appearance of SWNT’s comparable to that of MWCNTs was quite different. The individual tubes have very small diameters (typically ~ 1nm), and are curled and looped rather than straight. In the early 1990s, two research groups examined electronic properties of individual SWNTs. Many believe that Iijima's report in 1991 was of particular importance because it brought carbon nanotubes into the awareness of the scientific community as a whole.

1.5 TYPES OF NANOTUBES

1.5.1 Single Walled Carbon Nanotube

Single-walled nanotubes (SWNT) have a diameter of close to 1 nanometer, with a tube length that can be many millions of times longer. The structure of a SWNT can be conceptualized by wrapping a one-atom-thick layer of graphite called graphene into a seamless cylinder.

1.5.2 Multi Walled Carbon Nanotube

Multi-walled nanotubes (MWNT) consist of multiple rolled layers (concentric tubes) of graphene. There are two models that can be used to describe the structures of multi-walled nanotubes. In the Russian Doll model, sheets of graphite are arranged in concentric cylinders. In the Parchment model, a single sheet of graphite is rolled in around itself, resembling a scroll of parchment or a rolled newspaper. The interlayer distance in multi-walled nanotubes is close to the distance between graphene layers in graphite, approximately 3.4 Å. The Russian Doll structure is observed more commonly. Its individual shells can be described as SWNTs, which can be metallic or semiconducting. Because of statistical probability and restrictions on the relative diameters of the individual tubes, one of the shells, and thus the whole MWNT, is usually a zero-gap metal.

Double-walled carbon nanotubes (DWNT) form a special class of nanotubes because their morphology and properties are similar to those of SWNT but their resistance to chemicals is significantly improved. This is especially important when grafting of chemical functions at the surface of the nanotubes is required to add new properties to the CNT. In the case of SWNT, covalent functionalization will break some C=C double bonds, leaving "holes" in the structure on the nanotube and, thus, modifying both its mechanical and electrical properties. In the case of DWNT, only the outer wall is modified. DWNT synthesis on the gram-scale was first proposed in 2003 by the CCVD technique, from the selective reduction of oxide solutions in methane and hydrogen.

1.5.3 Torus

A nanotorus is a carbon nanotube bent into a torus (doughnut shape). Nanotori are predicted to have many unique properties, such as magnetic moments 1000 times larger than previously expected for certain specific radii. Properties such as magnetic moment, thermal stability, etc. vary widely depending on radius of the torus and radius of the tube.

1.5.4 Nanobud

Carbon nanobuds are a newly created material combining two previously discovered allotropes of carbon: carbon nanotubes and fullerenes. In this new material, fullerene-like "buds" are covalently bonded to the outer sidewalls of the underlying carbon nanotube. This hybrid material has useful properties of both fullerenes and carbon nanotubes. In particular, they have been found to be exceptionally good field emitters. In composite materials, the attached fullerene molecules may function as molecular anchors preventing slipping of the nanotubes, thus improving the composite's mechanical properties.

1.5.5 Graphenated Carbon Nanotubes (g-CNTs)

Graphenated CNTs are a relatively new hybrid that combines graphitic foliates grown along the sidewalls of multiwalled CNTs. Yu et al. reported on "chemically bonded graphene leaves" growing along the sidewalls of CNTs. Stoner et al. described these structures as "graphenated CNTs" and reported in their use for enhanced super capacitor performance. Hsu et al. further reported on similar structures formed on carbon fibre paper, also for use in super capacitor applications. The foliate density can vary as a function of deposition conditions (e.g. temperature and time) with their structure ranging from few layers of graphene (< 10) to thicker, more graphite-like.

The fundamental advantage of an integrated graphene-CNT structure is the high surface area three-dimensional framework of the CNTs coupled with the high edge density of graphene. Graphene edges provide significantly higher charge density and reactivity than the basal plane, but they are difficult to arrange in three-dimensional, high volume-density geometry. CNTs are readily aligned in high density geometry (i.e., a vertically aligned forest) but lack high charge density surfaces—the sidewalls of the CNTs are similar to the basal plane of graphene and exhibit low charge density except where edge defects exist. Depositing a high density of graphene foliates along the length of aligned CNTs can significantly increase the total charge capacity per unit of nominal area as compared to other carbon nanostructures.

1.5.6 Nitrogen Doped Carbon Nanotubes

Nitrogen doped carbon nanotubes (N-CNTs), can be produced through 5 main methods, Chemical Vapour Deposition, high-temperature and high-pressure reactions, gas-solid reaction of amorphous carbon with NH_3 at high temperature, solid reaction, and solvo thermal synthesis.

N-CNTs can also be prepared by a CVD method of pyrolysizing melamine under Ar at elevated temperatures of 800^{o}C - 980^{o}C. However synthesis via CVD and melamine results in the formation of bamboo structured CNTs. XPS spectra of grown N-CNTs reveals nitrogen in five main components, pyridinic nitrogen, pyrrolic nitrogen, quaternary nitrogen, and nitrogen oxides. Furthermore synthesis temperature affects the type of nitrogen configuration.

Nitrogen doping plays a pivotal role in Lithium storage. N-doping provides defects in the walls of CNTs allowing for Li ions to diffuse into interwall space. It also increases capacity by providing more favourable bind of N-doped sites. N-CNTs are also much more reactive to metal oxide nanoparticle deposition which can further enhance storage capacity, especially in anode materials for Li-ion batteries. However Boron doped nanotubes has been shown to make batteries with triple capacity.

1.5.7 Peapod

A Carbon peapod is a novel hybrid carbon material which traps fullerene inside a carbon nanotube. It can possess interesting magnetic properties with heating and irradiating. It can also be applied as an oscillator during theoretical investigations and predictions.

1.5.8 Cup-Stacked Carbon Nanotubes

Cup-stacked carbon nanotubes (CSCNTs) differ from other quasi-1D carbon structures, which normally behave as quasi-metallic conductors of electrons. CSCNTs exhibit semiconducting behaviours due to the stacking microstructure of graphene layers.

1.5.9 Extreme Carbon Nanotubes

The observation of the longest carbon nanotubes (18.5 cm long) was reported in 2009. These nanotubes were grown on Si substrates using an improved chemical vapour deposition (CVD) method and represent electrically uniform arrays of single-walled carbon nanotubes.

The shortest carbon nanotube is an organic compound cycloparaphenylene, which was synthesized in early 2009.

The thinnest carbon nanotube is armchair (2, 2) CNT with a diameter of 3 Å. This nanotube was grown inside a multi-walled carbon nanotube. Assigning of carbon nanotube type was done by combination of high-resolution transmission electron

microscopy (HRTEM), Raman spectroscopy and density functional theory (DFT) calculations.

The thinnest freestanding single-walled carbon nanotube is about 4.3 Å in diameter. Researchers suggested that it can be either (5, 1) or (4, 2) SWCNT, but exact type of carbon nanotube remains questionable. (3, 3), (4, 3) and (5, 1) carbon nanotubes (all about 4 Å in diameter) were unambiguously identified using aberration-corrected high-resolution transmission electron microscopy inside double-walled CNTs.

The highest density of CNTs was achieved in 2013, grown on a conductive titanium-coated copper surface that was coated with co-catalysts cobalt and molybdenum at lower than typical temperatures of 450 °C. The tubes averaged a height of 0.38 μm and a mass density of 1.6 g cm^{-3}. The material showed ohmic conductivity (lowest resistance ~22 kΩ).

1.6 PROPERTIES OF CARBON NANOTUBES

1.6.1 Strength

Carbon nanotubes are proved to be the strongest and stiffest materials due to the covalent sp^2 bonds formed between the individual carbon atoms. Due to this type of bonding, the strength results are more favourable in terms of tensile strength and elastic modulus. In 2000, a test was conducted on multi-walled carbon nanotube for tensile properties and the test was succeeded to have strength of 63 GPa and in 2008, tests revealed that individual CNT shells have strengths of up to 100 GPa, which is in agreement with quantum/atomistic models. As individual CNT shells possess extremely high strength, weak shear interactions between adjacent shells and tubes lowers the strength of multi-walled carbon nanotubes and carbon nanotube bundles only to few GPa's. This limitation has been recently addressed by applying high-energy electron irradiation, which crosslinks inner shells and tubes, and successfully increases the strength of these materials to 60 GPa for multi-walled carbon nanotubes and 17 GPa for double-walled carbon nanotube bundles.

1.6.2 Kinetic Properties

Multi-walled nanotubes are individual nanotubes shells placed concentrically within one another. These reveal a striking telescoping property whereby an inner nanotube core may slide, almost without friction, within its outer nanotube shell, thus possessing an atomically perfect linear or rotational bearing. The precise positioning of atoms of carbon to create useful machines is one of the true examples in molecular

nanotechnology. Already, this property has been utilized to create the world's smallest rotational motor. Future applications such as a gigahertz mechanical oscillator are also envisaged.

1.6.3 Electrical Properties

The unique electrical properties of carbon nanotubes are to a large extent derived from their 1-D character and the peculiar electronic structure of graphite. They have extremely low electrical resistance. Resistance occurs when an electron collides with some defect in the crystal structure of the material though which it is passing. The defect could be an impurity atom, a defect in the crystalline structure, or an atom vibrating about its position in the crystal. Such collisions deflect the electron from its path but the electrons inside a carbon nanotube are not so easily scattered because of their small diameter and huge ratio of length to diameter ratio that can be up in the millions or even higher.

1.6.4 Thermal Properties

CNT have now been shown to have thermal conductivity at least twice that of diamond. CNT have the unique property of feeling cold to the touch, like metal, on the sides with the tube ends exposed, but similar to wood on the other sides. The specific heat and thermal conductivity of carbon nanotubes systems are determined primarily by phonons. The measurements of the thermoelectric power (TEP) of nanotubes systems give direct information for the type of carriers and conductivity mechanisms.

1.6.5 Mechanical Properties

The carbon nanotubes are expected to have high stiffness and axial strength as a result of carbon-carbon sp^2 bonding. The practical application of the nanotubes requires the study of the elastic response, the inelastic behaviour and buckling, yield strength and fracture. Nanotubes are the stiffest known fibre, with a measured Young's modulus of 1.4 TPa and elongation to failure of 20–30%, which projects to a tensile strength of well above 100 GPa (possibly higher), by far the highest known. For comparison, the Young's modulus of high-strength steel is around 200 GPa, and its tensile strength is 1–2 GPa.

1.6.6 Toxicity

The toxicity of carbon nanotubes has been an important question in nanotechnology. The data are still fragmentary and subject to criticism. Preliminary results highlight the difficulties in evaluating the toxicity of this heterogeneous material. Parameters

such as structure, size distribution, surface area, surface chemistry, surface charge, and agglomeration state as well as purity of the samples, have considerable impact on the reactivity of carbon nanotubes. However, available data clearly show that, under some conditions, nanotubes can cross membrane barriers, which suggests that, if raw materials reach the organs, they can induce harmful effects such as inflammatory and fibrotic reactions. Under certain conditions CNTs can enter human cells and accumulate in the cytoplasm, can cause cell death. Results of rodent studies collectively show that regardless of the process by which CNTs were synthesized and the types and amounts of metals they contained, CNTs were capable of producing inflammation, epithelioid granulomas (microscopic nodules), fibrosis and biochemical/toxicological changes in the lungs. Comparative toxicity studies in which mice were given equal weights of test materials showed that SWCNTs were more toxic than quartz, which is considered a serious occupational health hazard when chronically inhaled. The needle-like fibre shape of CNTs is similar to asbestos fibres. This raises the idea that widespread use of carbon nanotubes may lead to pleural mesothelioma, a cancer of the lining of the lungs orperitoneal mesothelioma, a cancer of the lining of the abdomen.

1.7 SYNTHESIS

Techniques have been developed to produce nanotubes in sizable quantities, including arc discharge, laser ablation, high-pressure carbon monoxide disproportionation, and chemical vapour deposition (CVD). Large quantities of nanotubes can be synthesized by these methods; advances in catalysis and continuous growth are making CNTs more commercially viable.

1.7.1 Arc Discharge

Nanotubes were observed in 1991 in the carbon soot of graphite electrodes during an arc discharge, by using a current of 100 amps that was intended to produce fullerenes. However the first macroscopic production of carbon nanotubes was made in 1992 by two researchers at NEC's Fundamental Research Laboratory. The method used was the same as in 1991. During this process, the carbon contained in the negative electrode sublimates because of the high-discharge temperatures. Because nanotubes were initially discovered using this technique, it has been the most widely used method of nanotube synthesis.

1.7.2 Laser Ablation

In laser ablation, a pulsed laser vaporizes a graphite target in a high-temperature reactor while an inert gas is bled into the chamber. Nanotubes develop on the cooler surfaces of the reactor as the vaporized carbon condenses. A water-cooled surface may be included in the system to collect the nanotubes.

This process was developed by Dr. Richard Smalley and co-workers at Rice University, who at the time of the discovery of carbon nanotubes, were blasting metals with a laser to produce various metal molecules. When they heard of the existence of nanotubes they replaced the metals with graphite to create multi-walled carbon nanotubes. Later that year the team used a composite of graphite and metal catalyst particles (the best yield was from a cobalt and nickel mixture) to synthesize single-walled carbon nanotubes.

The laser ablation method yields around 70% and produces primarily single-walled carbon nanotubes with a controllable diameter determined by the reaction temperature. However, it is more expensive than either arc discharge or chemical vapour deposition.

1.7.3 Plasma Torch

Single-walled carbon nanotubes can be synthesized by the induction thermal plasma method, discovered in 2005 by groups from the University of Sherbrooke and the National Research Council of Canada. The method is similar to arc-discharge in that both use ionized gas to reach the high temperature necessary to vaporize carbon-containing substances and the metal catalysts necessary for the ensuing nanotube growth. The thermal plasma is induced by high frequency oscillating currents in a coil, and is maintained in flowing inert gas. Typically, a feedstock of carbon black and metal catalyst particles is fed into the plasma, and then cooled down to form single-walled carbon nanotubes. Different single-wall carbon nanotube diameter distributions can be synthesized.

The induction thermal plasma method can produce up to 2 grams of nanotube material per minute, which is higher than the arc-discharge or the laser ablation methods.

1.7.4 Chemical Vapour Deposition (CVD)

During CVD, a substrate is prepared with a layer of metal catalyst particles, most commonly nickel, cobalt, iron, or a combination. The metal nanoparticles can also be produced by other ways, including reduction of oxides or oxides solid solutions. The diameters of the nanotubes that are to be grown are related to the size of the metal

particles. This can be controlled by patterned (or masked) deposition of the metal, annealing, or by plasma etching of a metal layer. The substrate is heated to approximately 700°C. To initiate the growth of nanotubes, two gases are bled into the reactor: a process gas (such as ammonia, nitrogen or hydrogen) and a carbon-containing gas (such as acetylene, ethylene, ethanol or methane). Nanotubes grow at the sites of the metal catalyst; the carbon-containing gas is broken apart at the surface of the catalyst particle, and the carbon is transported to the edges of the particle, where it forms the nanotubes. This mechanism is still being studied. The catalyst particles can stay at the tips of the growing nanotube during growth, or remain at the nanotube base, depending on the adhesion between the catalyst particle and the substrate. Thermal catalytic decomposition of hydrocarbon has become an active area of research and can be a promising route for the bulk production of CNTs. Fluidised bed reactor is the most widely used reactor for CNT preparation. Scale-up of the reactor is the major challenge.

CVD is a common method for the commercial production of carbon nanotubes. For this purpose, the metal nanoparticles are mixed with a catalyst support such as MgO or Al_2O_3 to increase the surface area for higher yield of the catalytic reaction of the carbon feedstock with the metal particles. One issue in this synthesis route is the removal of the catalyst support via an acid treatment, which sometimes could destroy the original structure of the carbon nanotubes. However, alternative catalyst supports that are soluble in water have proven effective for nanotube growth.

If plasma is generated by the application of a strong electric field during growth (plasma-enhanced chemical vapour deposition), then the nanotube growth will follow the direction of the electric field. By adjusting the geometry of the reactor it is possible to synthesize vertically aligned carbon nanotubes (i.e., perpendicular to the substrate), a morphology that has been of interest to researchers interested in the electron emission from nanotubes. Without the plasma, the resulting nanotubes are often randomly oriented. Under certain reaction conditions, even in the absence of plasma, closely spaced nanotubes will maintain a vertical growth direction resulting in a dense array of tubes resembling a carpet or forest.

Of the various means for nanotube synthesis, CVD shows the most promise for industrial-scale deposition, because of its price/unit ratio, and because CVD is capable of growing nanotubes directly on a desired substrate, whereas the nanotubes must be

collected in the other growth techniques. The growth sites are controllable by careful deposition of the catalyst.

1.8 APPLICATIONS OF CARBON NANOTUBES

Carbon nanotubes (CNTs) are extensively used in various sectors like Energy, Medicine, Environment, Electronics and Civil Engineering applications.

- A team of researchers at Rice University have developed electrodes made from carbon nanotubes grown on graphene with very high surface area and very low electrical resistance. They have also built a solar cell that uses graphene as electrode while using buckyballs and carbon nanotubes to absorb light and generate electrons.
- Carbon nanotubes can also perform as a catalyst in a fuel cell by avoiding the use of expensive platinum on which most catalysts are based.
- Nanotubes and gold nanoparticles are used in sensors to detect proteins that indicate the presence of oral cancer. Also it can be used in improving the healing process for broken bones by providing a carbon nanotube scaffold that new bone material can grow around, using nanotubes as a cellular scale needle to deliver quantum dots and proteins into cancer cells.
- As CNTs have high strength and flexibility, so their use also exist in aircraft industry which includes highly stressed components, a lightweight, low power anti-icing system.
- Cables made from carbon nanotubes are strong enough to be used in building the Space Elevator to drastically reduce the cost of lifting people and materials into orbit.
- CNTs also have tremendous range of applications in concrete structures depending on the size and morphology of the fibrous carbons. As the size of CNT particles is finer than cement particles, so these can be used in concrete as void filler. On the other hand, we could say carbon nanotubes/nanofibres (CNTs/CNFs) are used as nano-reinforcements in cement-based materials.
- For load-bearing applications, CNT powders mixed with polymers or precursor resins can increase stiffness, strength, and toughness. These enhancements depend on CNT diameter, aspect ratio, alignment, dispersion, and interfacial interaction with the matrix.

- CNTs are also applicable to be used as additives in the organic precursors used to form carbon fibres which have been used as reinforcements in high strength, light weight, high performance composites. Theoretical studies have suggested that SWNTs could have a Young's modulus as high as 1TPa, which is basically the in-plane value of defect free graphite.
- Apart from strength characteristics nanotubes have shown promise in enhancing the mechanical performance, the resistance to chloride penetration, and the self-compacting properties of concrete and in reducing permeability and shrinkage. The most important application of nanotubes based on their mechanical properties will be as reinforcements in composite materials.
- Makar et al. were among the first to indicate, using hardness measurements, that CNTs can affect early-age hydration and that a strong bond is possible between the cement paste and the CNTs. The main problem is in creating a good interface between nanotubes and the polymer matrix and attaining good load transfer from the matrix to the nanotubes, during loading. The reason for this is essentially twofold. First, nanotubes are atomically smooth and have nearly the same diameters and aspect ratios (length/diameter) as polymer chains. Second, nanotubes are almost always organized into aggregates which behave differently in response to a load, as compared to individual nanotubes.
- The small and uniform dimensions of the nanotubes produce some interesting applications. With extremely small sizes, high conductivity, high mechanical strength and flexibility (ability to easily bend elastically), nanotubes may ultimately become necessary in their use as nanoprobes.
- Nowadays, researches have been carried out in using nanotubes as sensors embedded in the concrete structures as crack detectors.
- It has a wide range of scope in health monitoring applications of concrete structures as well. Apart from these applications the major challenges that are being faced in its usage are their availability and cost. For bulk applications, such as fillers in composites, where the atomic structure has a much smaller impact on the resulting properties, the quantities of nanotubes that can be manufactured still falls far short of what industry would need. The market price of nanotubes is also too high presently for any realistic commercial application. But it should be noted that the starting prices for carbon fibres and fullerenes were also prohibitively high during their initial stages

of development, but have come down significantly in time. If CNTs are made easily available in the market then they are prove to be the most innovative and advantageous material in relation to concrete structures.

1.9 FLY ASH

Fly ash is one of the most extensively used by-product material in the construction field resembling Portland cement (Pfeifer, 1969). It is an inorganic, non combustible, finely divided residue collected or precipitated from the exhaust gases of any industrial furnace (Halstead, 1986). Most of the fly ash particles are solid spheres and some particles called cenospheres are hollow (Kosmatka et al., 2002). Also present are plerospheres which are spheres containing smaller spheres inside. The particle size in fly ash varies from less than 1µm to more than 100µm with the typical particle size measuring less than 20µm. Their surface area is typically 300 to 500 m^2/kg, although some fly ashes can have surface areas as low as 200 m^2/kg and as high as 700 m^2/kg. Fly ash is primarily silicate glass containing silica, alumina, iron and calcium. The relative density or specific gravity of fly ash generally ranges between 1.9 and 2.8 and the colour is generally gray or tans (Halstead, 1986).

1.9.1 Classification of Fly Ash

ASTM- C 618-93 categorizes natural pozzolans and fly ashes into the following three categories:-

1. **Class N Fly Ash:** Raw or calcined natural pozzolans such as diatomaceous earths, opaline chert and shale, stuffs, volcanic ashes and pumice come in this category. Calcined kaolin clay and laterite shale also fall in this category of pozzolans.
2. **Class F Fly Ash:** Fly ash normally produced from burning anthracite or bituminous coal falls in this category. This class of fly ash exhibits pozzolanic property but rarely if any, self hardening property.
3. **Class C Fly Ash:** Fly ash normally produced from lignite or sub-bituminous coal is the only material included in this category. This class of fly ash has both pozzolanic and varying degree of self cementitious properties. (Most Class C fly ash ashes contain more than 15% CaO. But some Class C fly ashes may contain as little as 10% CaO).

Table 1.1 Requirements for Fly Ash and Natural Pozzolans for use as a Mineral Admixture in Portland Cement Concrete as per ASTM C 618-93

Requirements	Fly ash classifications		
	N	F	C
Chemical Requirements			
SiO_2+Al_2O_3+Fe_2O_3, min%	70	70	70
SO3, max%	4	5	5
Moisture content, max%	3	3	3
Loss on ignition, max%	10	6	6

Physical requirements			
Amount retained when wet sieved on 45mm sieve, max%	34	34	34
Pozzolanic activity index, with Portland cement at 28 days, min% of control	75	75	75
Pozzolanic activity index, with lime at 7 days, min (MPa)	5.5	5.5	-
Water requirement, max% of control	115	105	105
Autocalve expansion or contraction, max	0.8	0.8	0.8
Specific gravity	5	5	5
Percentage retained on 45 mm sieve	5	5	5

1.10 OBJECTIVE OF RESEARCH

In the present study, the effect of addition of different percentages of CNTs in concrete on mechanical properties and durability of concrete are examined. In all concrete mixes (except control mix) 20 percent fly ash is added at replacement of cement by weight. The objectives of the work are as under.

1) To study the effect of addition of CNTs and fly ash on compressive strength of concrete.
2) To study the effect of addition of CNTs and fly ash on splitting tensile strength of concrete.

3) To study the effect of addition of CNTs and fly ash on young's modulus of concrete.
4) To study the effect of addition of CNTs and fly ash on permeability of concrete.

1.11 ORIENTATION OF THESIS

The thesis report consists of five chapters:

Chapter 1- Provides introduction about Carbon nanotubes and fly ash, their properties, synthesis, applications etc.

Chapter 2- Deals with the study of various researchers on CNTs and Fly Ash and their effect on different mechanical as well as durability properties.

Chapter 3- Details the scheme of experimentation, materials used and variables involved. Information about concrete mix designs is also illustrated in this chapter.

Chapter 4- Presents the results, and their analysis for the strength properties such as compressive strength, splitting tensile strength, modulus of elasticity and durability property such as rapid chloride permeability test.

Chapter 5- Summarizes and concludes the findings of the study. Few recommendations for further studies are also discussed.

References are placed at the end.

1.12 SUMMARY

This chapter discussed about the (i) types, properties, applications of CNTs in civil engineering work, (ii) different synthesis methods adopted, (iii) objective of thesis and (iv) orientation of thesis.

CHAPTER 2

LITERATURE REVIEW

2.1 PRELIMINARY REMARKS

Nanotechnology is a science in its growing stage. In general, all of today's practical nanotechnologies are those using nanosized particles in so-called nanomaterials and nanometer-size features on integrated circuits. In the world of nanotechnology, nanomaterials either referred to as materials with nanoscale dimensions or bulk materials containing nanosized particles. Nanoparticles are defined as particles whose diameter is less than 100 nm. These materials exhibit various characteristics such as extraordinary strength or unsuspected electrical, physical or chemical properties that are completely different from those demonstrated by the same products with larger dimensions. The reason behind this is the increased relative surface area of minute particles. The unique multification properties of carbon nanotubes make them promising reinforcements to many engineering materials. CNTs occur in two forms either as single-walled carbon nanotubes (SWCNTs) or as multi-walled carbon nanotubes (MWCNTs). SWCNTs are composed of a single graphite sheet rolled into a long hollow cylinder, whereas MWCNTs are formed by positioning SWCNTs concentrically one over the other. The average diameter of an individual SWCNT is on the order of 1 nm whereas the average diameter of an individual MWCNT is on the order of 10 nm. Their density is less than that of steel or glass fibre and also has an elastic modulus in the range of terapascal and yield strength of approximately 20–60 GPa, and yield strain of up to 10%.

2.2 MECHANICAL PROPERTIES

2.2.1 Compressive Strength

Sathawane et al. (2013) detailed the combine effect of rice husk ash and fly ash on concrete by 30% cement replacement. In this test, the combine proportion started from 30% FA and 0% RHA mix together in concrete by replacement of cement with the gradual increase of RHA by 2.5% and simultaneously gradual decrease of FA by 2.5%. The concrete specimens were tested after 7, 14, 28, 56 and 90 days of curing as per IS: 516-1959. Their mix proportion shown as:

Table 2.1 Concrete Mix Proportions (Sathawane et al., 2013)

Material	Quantity	Proportion
Cement	435.45 kg/m^3	1
Sand	476 kg/m^3	1.1
Coarse Aggregates	1242.62 kg/m^3	2.85
Water	191.6 kg/m^3	0.44
Slump	75-100 mm	----

Table 2.2 Results of Compressive Strength with different % of FA+RHA (Sathawane et al., 2013)

S. no.	Mix proportion		Compressive strength after no. Of days of curing in MPa				
	FA by % of cement	RA by % of cement	7 days	14 days	28 days	56 days	90 days
1	Control mixture		35.56	39.11	45.78	48	49.78
2	30	0	32.89	33.33	39.11	42.22	44.89
3	27.5	2.5	31.11	31.33	35.11	37.33	39.56
4	25	5	31.56	32.44	40.44	43.11	45.78
5	22.5	7.5	22.67	34.67	41.78	44.89	46.67
6	20	10	22.22	26.22	33.78	35.11	37.78
7	17.5	12.5	18.22	24.89	33.78	32.00	34.67
8	15	15	17.78	24.00	28.89	30.67	33.78

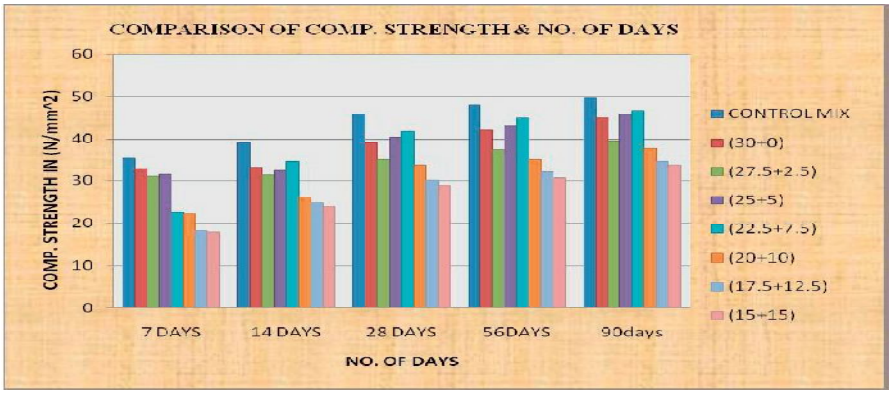

Fig. 2.1 Comparison of Compressive Strength for different % of RHA and FA (Sathawane et al., 2013)

Based on the above results, it was concluded that the compressive strength increases with increase in the percentage of Fly Ash and Rice Husk Ash up to replacement (22.5% FA and7.5%% RHA) of cement in concrete for different mix proportions.

Nassar et al. (2013) studied field investigation of high-volume fly ash pavement concrete. For performing this test, cores were drilled from pavement and were tested after 270 days of concrete age. High volume fly ash was adopted as a partial replacement in pavement so as to produce durable infrastructure and above all to have an economic concrete pavements. Type 1 Portland cement and Class C fly ash was used for the test. Two types of concrete mix designs were prepared. In control mix, 25% replacement of cement with class C fly ash was made, whereas in HVFA mix 50% replacement was made.

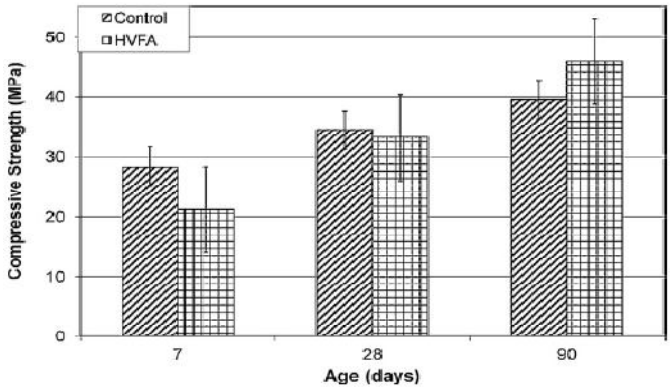

Fig. 2.2 Compressive Strength Test Results of Eastbound Pavement Concrete Specimens (Nassar et al., 2013)

Fig. 2.2 made clear that up to the age of 28 days the compressive strength of HVFA concrete mixture was less as compared to the control mixture. But the trend was opposite at the age of 90 days. The reason behind this was that at the age of 90 days, the pozzolanic reaction of fly ash with cement hydrates increases resulting in microstructural improvements of hydrated cement paste.

Siddique et al. (2012) investigated the influence of water/powder ratio on strength properties of self-compacting concrete containing coal fly ash and bottom ash. SCC was made with coal bottom ash as replacement of fine aggregates with varying percentages of 0%, 10%, 20% and 30% and fly ash was also used in replacement with cement at 15-35%. The concrete specimens were tested at the ages of 28, 90 and 365 days for various mixes. OPC 43 grade cement and Class F Fly ash were used. The compressive strength for various mixes with bottom ash percentages varying from 0 to 30% was shown in fig. 2.3, 2.4, 2.5 and 2.6.

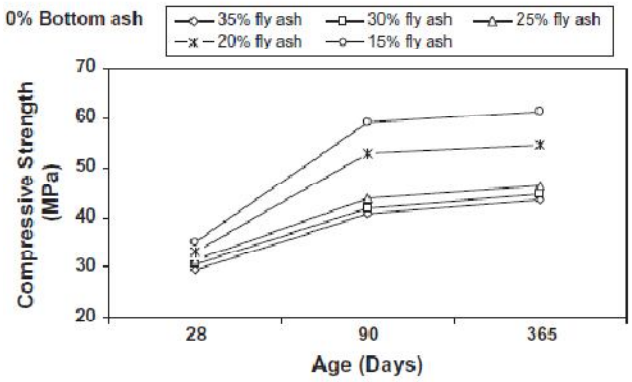

Fig. 2.3 Compressive Strength (0% Bottom Ash) at Various Fly Ash Contents (Siddique et al., 2012)

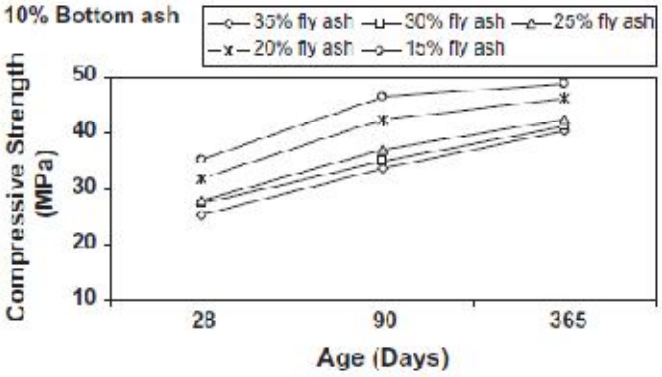

Fig. 2.4 Compressive Strength (10% Bottom Ash) at various Fly Ash Contents (Siddique et al., 2012)

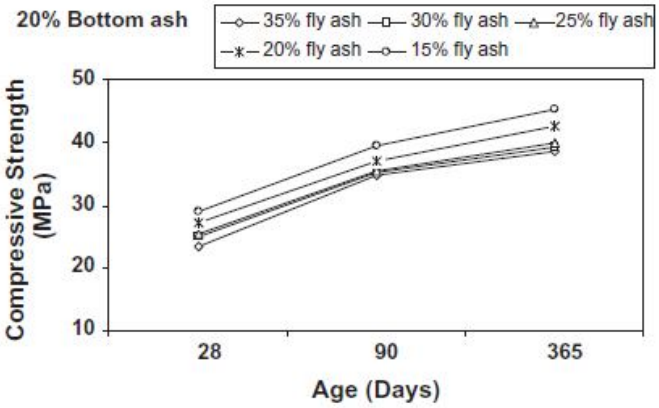

Fig. 2.5 Compressive Strength (20% Bottom Ash) at various Fly Ash Contents (Siddique et al., 2012)

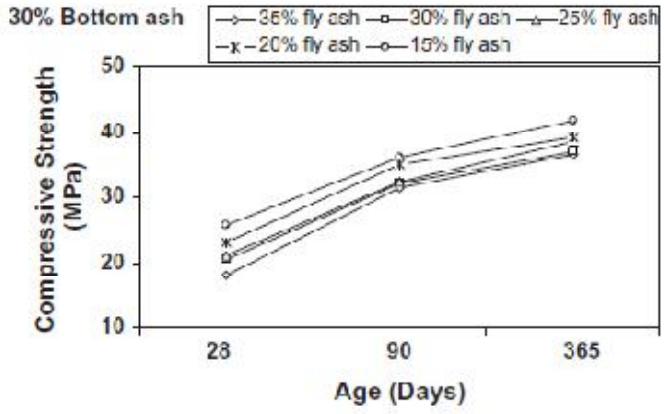

Fig. 2.6 Compressive Strength (30% Bottom Ash) at various Fly Ash Contents (Siddique et al., 2012)

From the figures mentioned above, it proved that the compressive strength increases with age. It was also observed that at 35% replacement, the compressive strength reduces as compared to the control mixture shown in fig. 2.3.

Dehwah (2012) studied the mechanical properties of self-compacting concrete incorporating quarry dust powder, silica fume or fly ash. This test was performed to assess the proportions of Quarry dust powder (QDP), QDP + SF or FA required for producing SCC flow criteria. A polycarboxylic ether based plasticizer was also used that greatly improves cement dispersion and provides flowable concrete. Cube specimens of 100x100x100 mm were used for calculating the compressive strength after 7, 14, 28 and 90 days of curing.

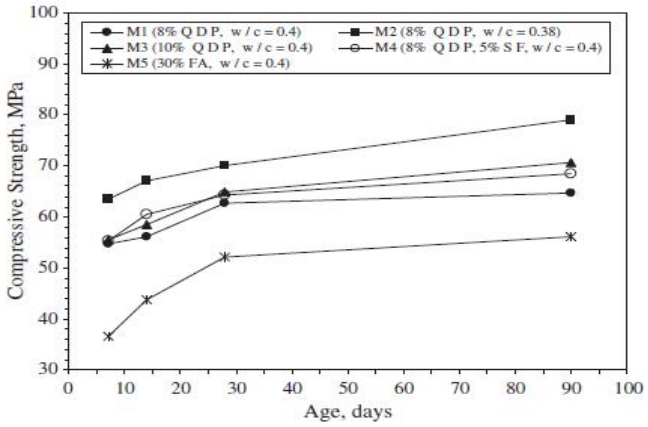

Fig. 2.7 Compressive Strength Variation with Age in the SCC Specimens (Dehwah, 2012)

Fig. 2.7 clearly justified that the compressive strength was maximum in the mix M2 (8% QDP, w/c = 0.38). The compressive strength for all mixes increased significantly. But the mixes in which only QDP was used showed the better results as

compared to the mixes in which SF+QDP or FA were used. This indicated that 8-10% QDP acted as better filler than FA or QDP+SF.

Boga and Topcu (2012) investigated the influence of fly ash on corrosion resistance and chloride ion permeability of concrete. In this study, fly ash with varying percentages like 0%, 15%, 30% and 45% was used in replacement to CEM 1 42.5R cement to evaluate the compressive strength of concrete. The samples were tested for 28 and 56 days in two different conditions i.e air and water. 150x150x150 mm cube specimens were prepared for investigating compressive strength.

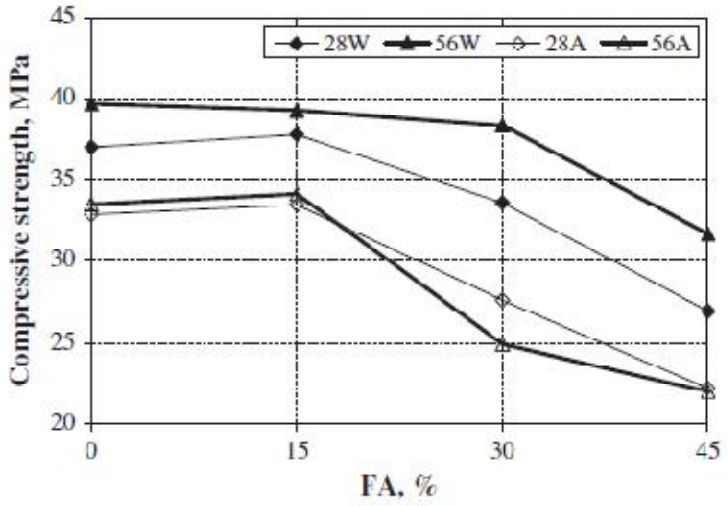

Fig. 2.8 Compressive Strength with varying Fly Ash Ratios

(Boga and Topcu, 2012)

Under water curing conditions, compressive strength after 56 days showed better results due to lengthening of cure conditions as compared to 28W. Similar is the case for air curing conditions, due to lengthening of cure conditions, compressive strength at 56 days showed better results as compared to 28 days because at later ages, fly ash added reacts with $Ca(OH)_2$ which in turn, formation of new CSH gel took place and hence the bonding get enhanced.

Karahan and Atis (2011) investigated the durability properties of polypropylene fiber reinforced fly ash concrete. Fly ash content used in the mix was 0%, 15%, and 30% in mass basis and fiber volume fraction was 0%, 0.05%, 0.10% and 0.20% in volume basis. A polycarboxylic ether based plasticizer i.e. 1% of the cement content was used.

Table 2.3 Mix Proportion (Karahan and Atis, 2011)

Mixture	PC (kg/m^3)	Fly ash (kg/m^3)	PP fiber (kg/m^3)	W (lt/m^3)	HP (kg/m^3)	Aggr. (kg/m^3)
A1	400	-	-	140	4.0	1891
A2	400	-	0.45	140	4.0	1890
A3	400	-	0.90	140	4.0	1889
A4	400	-	1.80	140	4.0	1886
B1	340	60	-	140	4.0	1874
B2	340	60	0.45	140	4.0	1872
B3	340	60	0.90	140	4.0	1871
B4	340	60	1.80	140	4.0	1868
C1	280	120	-	140	4.0	1856
C2	280	120	0.45	140	4.0	1855
C3	280	120	0.90	140	4.0	1853
C4	280	120	1.80	140	4.0	1851

Table 2.4 Compressive strength results (Karahan and Atis, 2011)

S.no.	Compressive strength (MPa)	S.no.	Compressive strength (MPa)	S.no.	Compressive strength (MPa)
A1	63.4	B1	52.9	C1	45.3
A2	64.9	B2	52.0	C2	43.0
A3	62.2	B3	53.6	C3	42.4
A4	61.5	B4	49.5	C4	44.3

Table 2.4 justified that the compressive strength decreased with the increase of fly ash. On the other hand, there was slight reduction in compressive strength even by the addition of polypropylene fibers. This was attributed by the redistribution of void structure due to the inclusion of fiber and the presence of weak interfacial bonds between the fiber and cement-fly ash grains.

Shuang (2011) studied the influence of fly ash on the mechanical properties of frame concrete. The study made in this experiment was carried out over water-binder ratios ranging from 0.30 to 0.42 and fly ash-binder ratios from 0% to 30%, based on

concrete framework model theory. The compressive and flexural strengths were determined after 28 days, 56 days and 90 days.

The results of compressive strength at different w/c ratios and with different replacements of fly ash by weight with cement were shown in fig. 2.9, 2.10, 2.11, and 2.12 as:

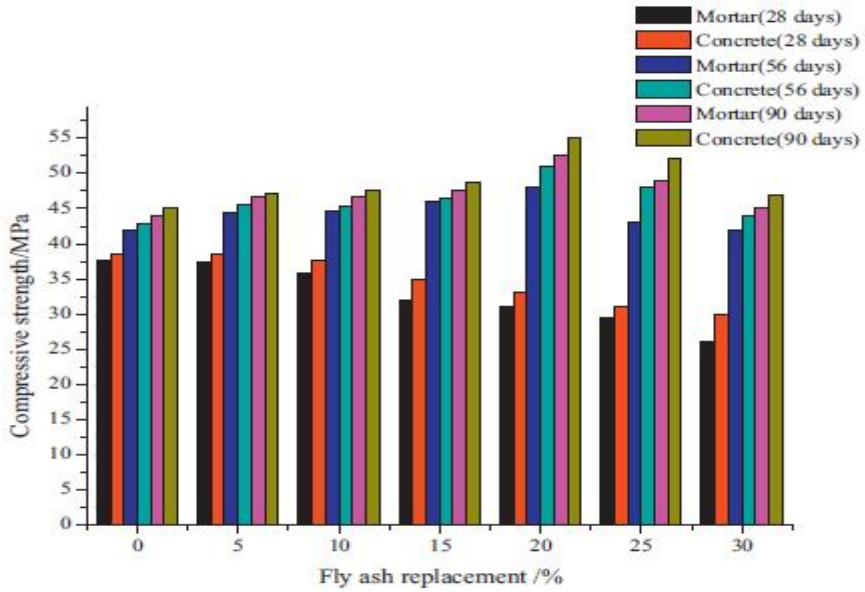

Fig.2.9 Relationship between Compressive Strength and Percentage Replacement of Fly Ash (w/cm=0.42) (Shuang, 2011)

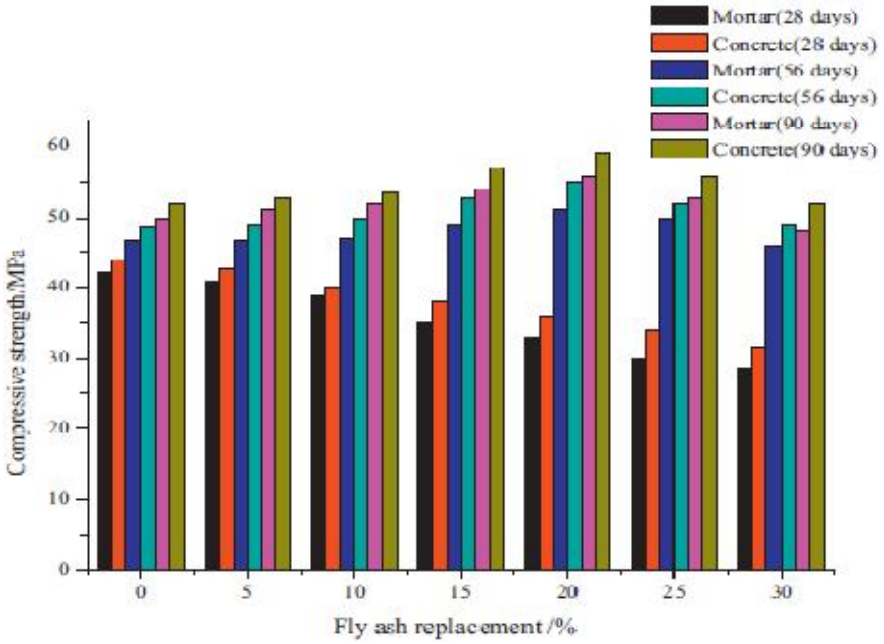

Fig.2.10 Relationship between Compressive Strength and Percentage Replacement of Fly Ash (w/cm=0.38) (Shuang, 2011)

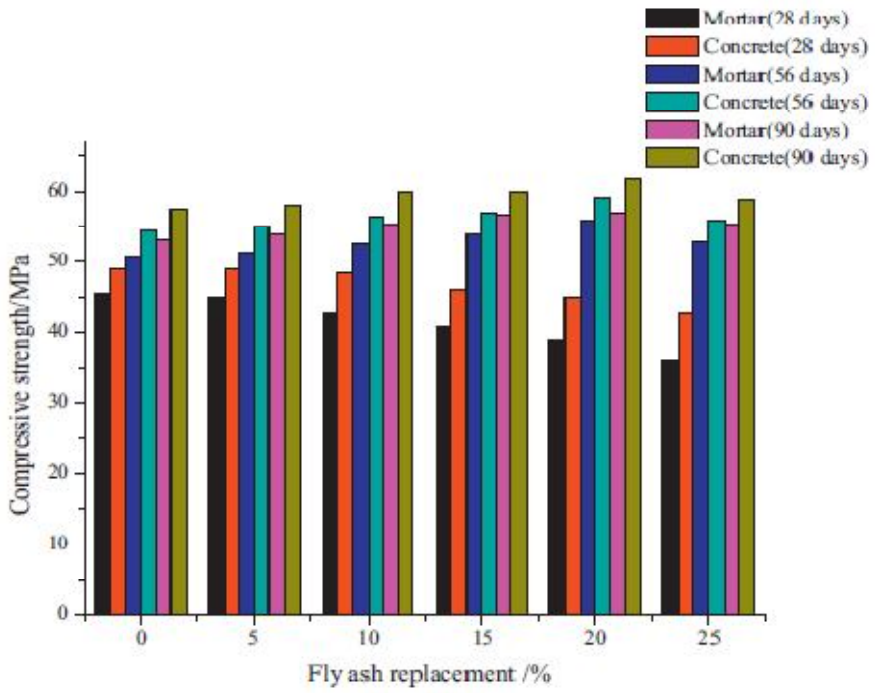

Fig.2.11 Relationship between Compressive Strength and Percentage Replacement of Fly Ash (w/cm=0.34) (Shuang, 2011)

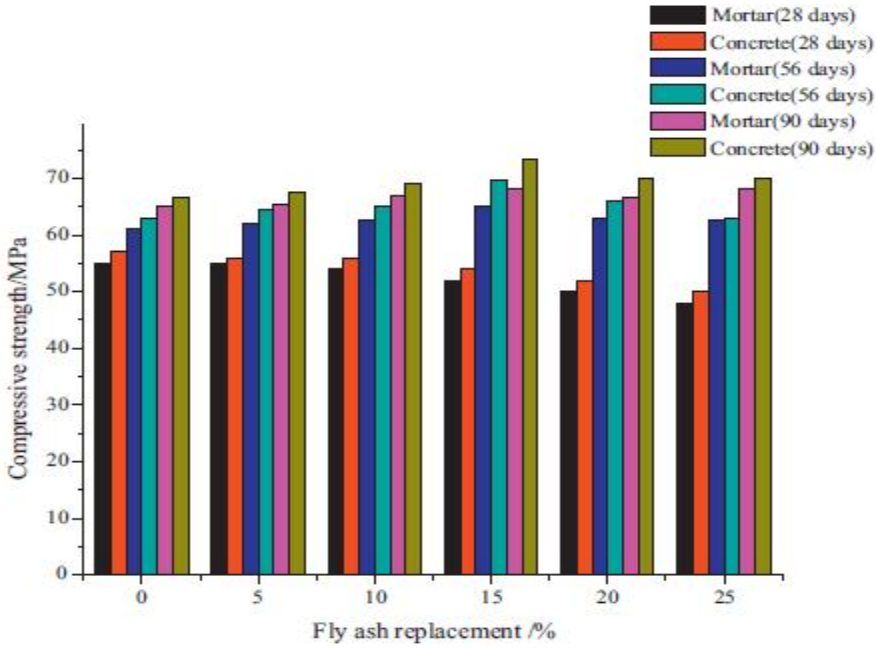

Fig.2.12 Relationship between Compressive Strength and Percentage Replacement of Fly Ash (w/cm=0.30) (Shuang, 2011)

Data from the figures above clearly showing that the 28 day compressive strength and its corresponding mortar matrix was lower than that of control concrete and its corresponding mortar matrix, but there was increase in strength after 56 days and 90 days. The reason behind this is as:

When fly ash is mixed with water, together with cement, it induces pozzolanic reaction, in which glass phase silica (SiO_2) and alumina (Al_2O_3) progressively react with $Ca(OH)_2$ formed by cement hydration, forming hydrates of calcium silicate. This reduces the $Ca(OH)_2$ content, which is weakness in concrete strength, while increasing C–S–H gel, which is responsible for the formation of structure of hardened cement. Therefore, in concrete containing fly ash, the hydration of cement forms the hardened structure, and the pozzolanic reaction of fly ash. The reaction of SiO_2 and Al_2O_3 in fly ash depends on the concentration and content of $Ca(OH)_2$ supply. The higher the $Ca(OH)_2$ concentration, the higher the rate of pozzolanic reaction. At the late ages, the higher the $Ca(OH)_2$ content, the longer that the pozzolanic reaction of fly ash lasts.

Chaipanich et al. (2010) investigated the compressive strength and microstructure of carbon nanotubes-fly ash cement composites. In this experiment, carbon nanotubes of 0.5% and 1% by weight were added in a fly ash cement system to produce carbon nanotubes–fly ash composites in the form of pastes and mortars. The mix proportion of carbon nanotubes-fly ash cement composites adopted is shown in table 2.5 as:

Table 2.5 Mix Proportions of Carbon Nanotubes-Fly Ash Cement Composites (Chaipanich et al., 2010)

Mix	PC (%)	FA (%)	CNT (%)	w/c
PC	100	-	-	0.5
FA20	80	20	-	0.5
FA20:CNT0.5	80	20	0.5	0.5
FA20:CNT1	80	20	1	0.5

The ratio of water: cement blends: sand used was 0.5: 1: 3 for all mixes. The specimens were tested after 7, 28 and 60 days and the corresponding results were shown in fig. 2.13.

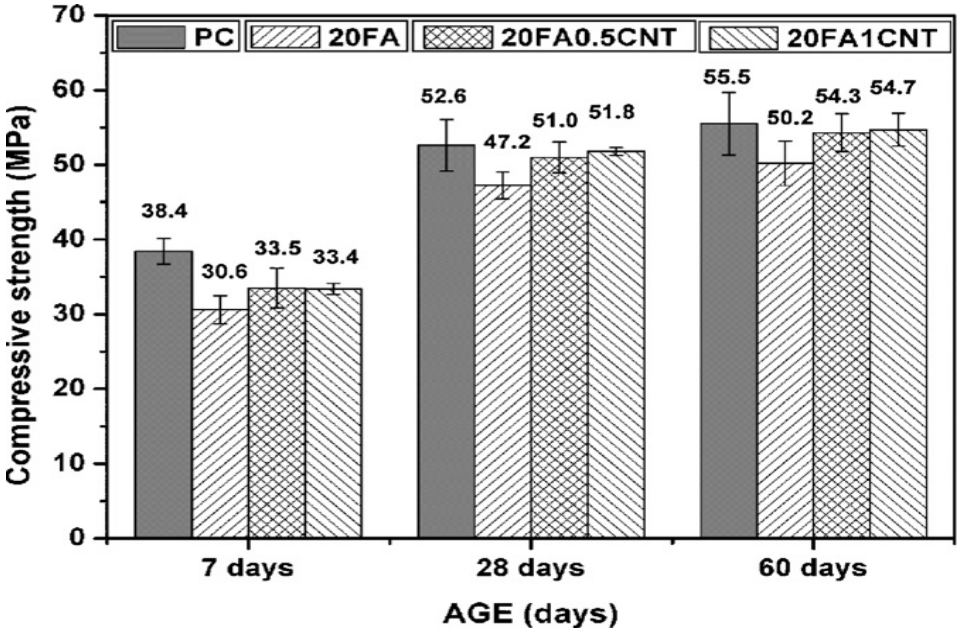

Fig.2.13 Compressive Strength of Carbon Nanotubes-Fly Ash Cement Composites at 7, 28 and 60 days (Chaipanich et al., 2010)

Results shown in fig.2.13 demonstrate that the compressive strength was found to increase with increasing carbon nanotubes content. The highest strength was found at 1% CNT content by weight. The higher strength of these fly ash–carbon nanotubes mortars was found because CNT particles has finer size as compared to cement particles and hence can further fill in the pores between the hydration products such as calcium silicate hydrates (CSH) and ettringite. From the above results, it was also concluded that the increase in compressive strength by addition of CNTs to the mix was only due to the physical improvement and not by any chemical interaction between the FA cement matrix and CNTs.

Topcu and Canbaz (2007) studied the effect of different fibers on the mechanical properties of concrete containing fly ash. In this test, the cement was replaced by weight with 10%, 15% and 20% of fly ash and effects of addition of steel and polypropylene fibers were experimentally investigated. Use of fly ash provides economical advantages to the production of concrete. The fibers used in concrete provide better performance whereas, on the other hand fly ash adjusted the workability and strength losses caused by fibers, and improve strength gain. The cement used in the experiment was ASTM Type 1 Portland cement. The fly ash used was Class F type fly ash and fibers with both ends twisted which belong to C type were used.

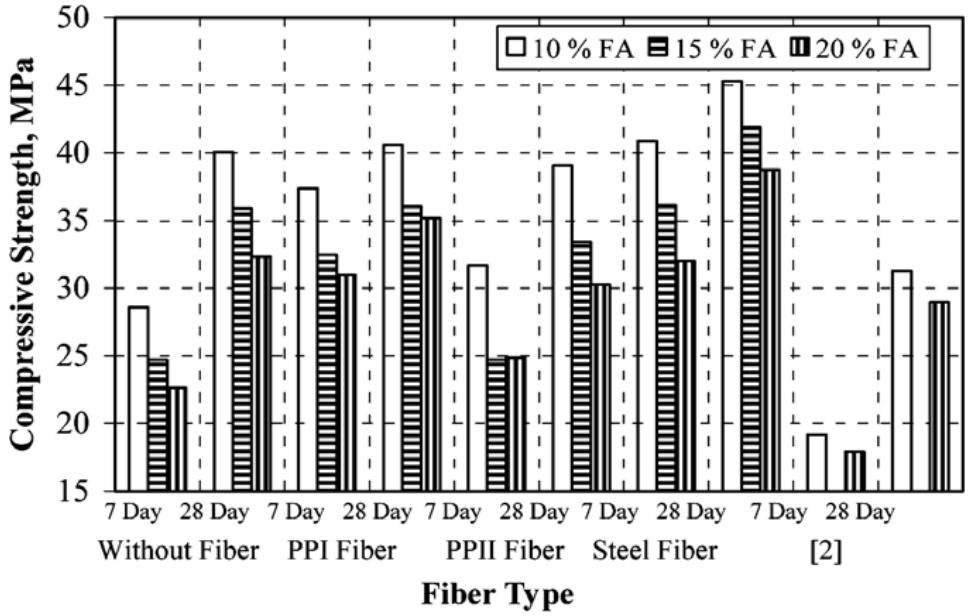

Fig.2.14 Cylindrical Compressive Strength versus Fiber Type (Topcu and Canbaz, 2007)

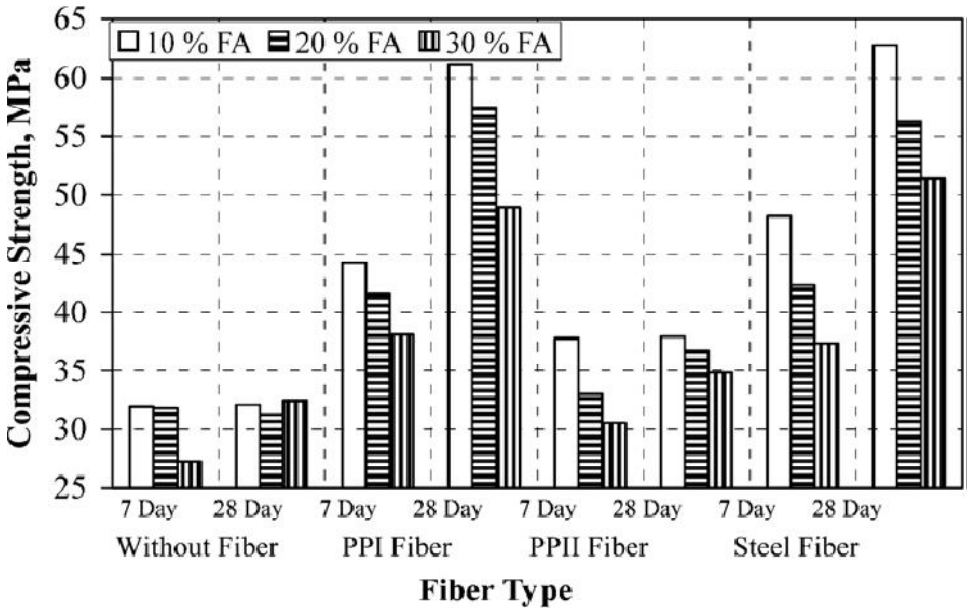

Fig.2.15 Cubic Compressive Strength versus Fiber Type (Topcu and Canbaz, 2007)

Fig.2.14 and fig.2.15 was clearly showing that the compressive strength of concrete produced with fibers was increased as compared to concrete produced without fibers. However, there was a decrease of 6% at 28 day compressive strength of cylinder concrete specimen produced with PPII fiber. The compressive strengths of concrete specimens were decreased as the fly ash content was used in concrete mixture. Fibers used in concrete helped by reducing the crack formation under axial loads and thus the compressive strength got increased. Tensile strength of PPII fiber is lower than

PPI and steel fibers. For this reason, the adherence and the compressive strength of concrete made with PPII decrease compared to PPI containing concrete. FA retards the strength development of concrete when replace with cements. Therefore, compressive strength of 7 and 28 days concrete specimens were decreased related to FA ratio. The relative strengths of cylindrical and cubical specimens shown as:

Table 2.6 Relative Strength of Concrete (Topcu and Canbaz, 2007)

Series	Relative compressive strength (%)			
	7 day cyl.	28 day cyl.	7 day cube	28 day cube
A1	100	100	100	100
A2	131	101	138	190
A3	111	97	118	118
A4	143	113	151	195
B1	86	89	100	97
B2	114	90	130	179
B3	87	83	103	114
B4	126	105	132	175
C1	79	81	85	101
C2	108	88	119	152
C3	87	76	95	108
C4	112	97	117	160

2.2.2 Split Tensile Strength

Sathawane et al. (2013) detailed the combine effect of rice husk ash and fly ash on concrete by 30% cement replacement. In this test, the combine proportion started from 30% FA and 0% RHA mix together in concrete by replacement of cement with the gradual increase of RHA by 2.5% and simultaneously gradual decrease of FA by 2.5%. The concrete specimens were tested after 7, 14, 28, 56 and 90 days of curing as per IS: 516-1959.

Table 2.7 Results of Split Tensile Strength with different % Of FA+RHA at 28 days of Curing (Sathawane et al., 2013)

S.no.	Mix proportion		Split tensile strength after 28 days of curing in MPa
	FA by % of cement	RHA by % of cement	
1	Control mix		4.38
2	30	0	4.10
3	27.5	2.5	3.82
4	25	5	3.67
5	22.5	7.5	3.96
6	20	10	2.97
7	17.5	12.5	2.26
8	15	15	1.98

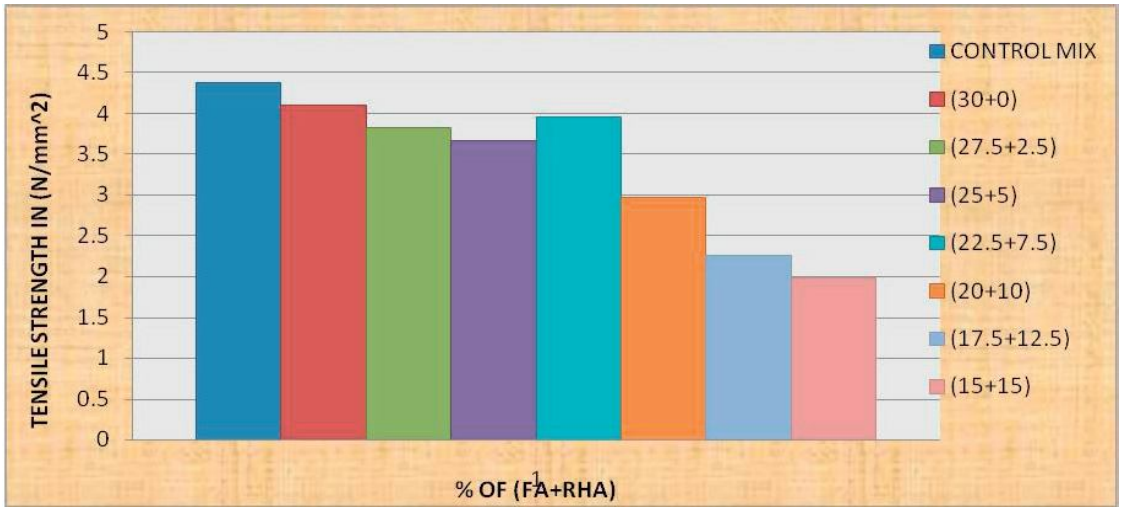

Fig.2.16 Comparison of Split Tensile Strength for different % Of RHA and FA at 28 days of Curing (Sathawane et al., 2013)

From fig. 2.16, it was observed that split tensile strength at the combination of 22.5% FA and 7.5% RHA decreases by 9.58% as compared to control concrete at 28 days of curing.

Siddique et al. (2012) investigated the influence of water/powder ratio on strength properties of self-compacting concrete containing coal fly ash and bottom ash. SCC was made with coal bottom ash as replacement of fine aggregates with varying percentages of 0%, 10%, 20% and 30% and fly ash was also used in replacement with cement at 15-35%. The concrete specimens were tested at the ages of 28, 90 and 365

days for various mixes. OPC 43 grade cement and Class F Fly ash were used. The split tensile strength for various mixes with bottom ash percentages varying from 0 to 30% was shown in fig. 2.17, 2.18, 2.19 and 2.20.

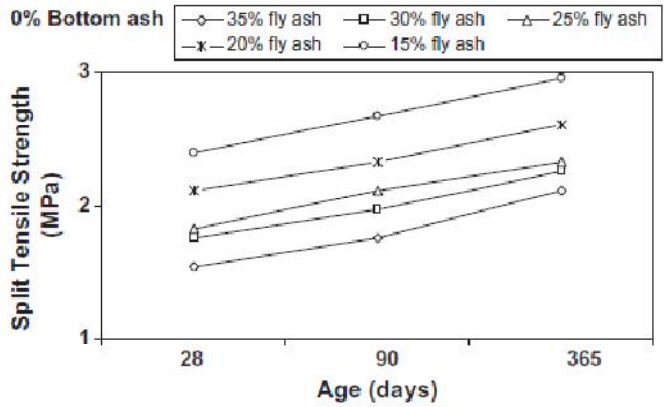

Fig. 2.17 Split Tensile Strength (0% Bottom Ash) at various Fly Ash Contents (Siddique et al., 2012)

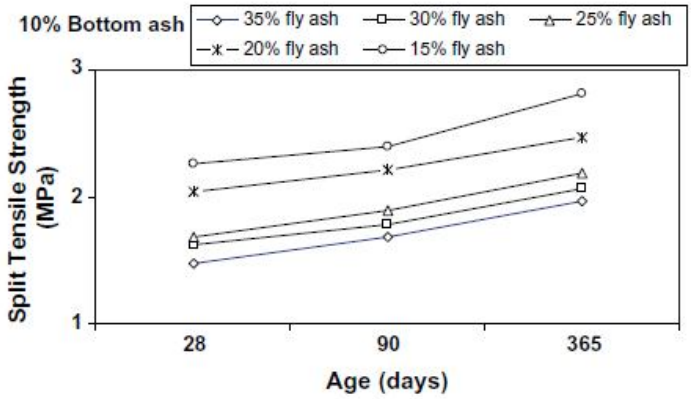

Fig. 2.18 Split Tensile Strength (10% Bottom Ash) at various Fly Ash Contents (Siddique et al., 2012)

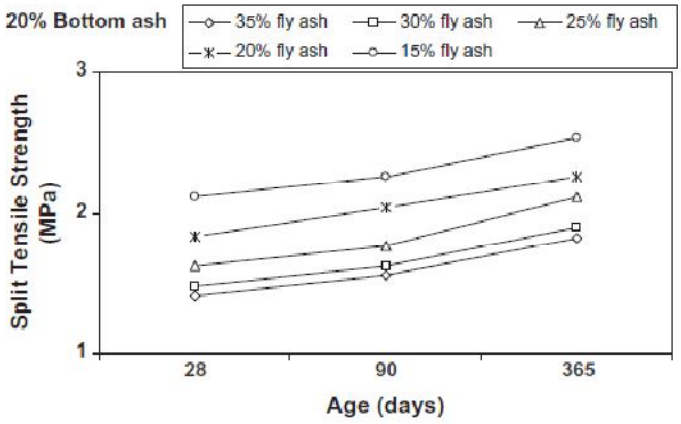

Fig. 2.19 Split Tensile Strength (20% Bottom Ash) at various Fly Ash Contents (Siddique et al., 2012)

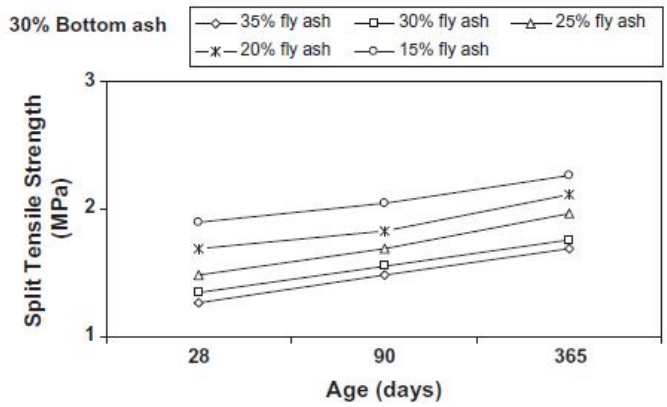

Fig. 2.20 Split Tensile Strength (30% Bottom Ash) at various Fly Ash Contents (Siddique et al., 2012)

From the figures mentioned above, it proved that the split tensile strength increases with age. It was also observed that at 35% replacement, the split tensile strength reduces as compared to the control mixture shown in fig. 2.17.

Dehwah (2012) studied the mechanical properties of self-compacting concrete incorporating quarry dust powder, silica fume or fly ash. This test was performed to assess the proportions of Quarry dust powder (QDP), QDP + SF or FA required for producing SCC flow criteria. A polycarboxylic ether based plasticizer was also used that greatly improves cement dispersion and provides flowable concrete. Cylinderical concrete specimens 75 mm in diameter and 150 mm high were prepared for evaluating the split tensile strength after 28 days of curing. The various mixes used were M1 (8% QDP, w/c = 0.40), M2 (8% QDP, w/c = 0.38), M3 (10% QDP, w/c = 0.40), M4 (8% QDP plus 5% SF, w/c = 0.40), and M5 (30% FA, w/c = 0.40).

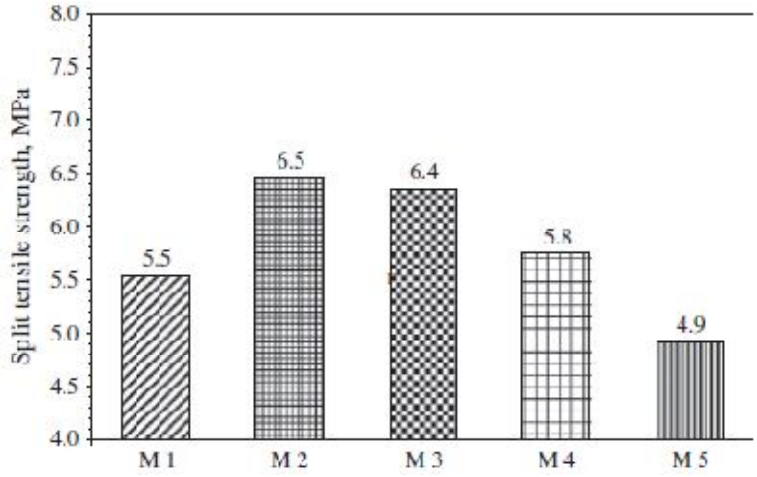

Fig. 2.21 Split Tensile Strength of SCC Specimens after 28 days of Curing (Dehwah, 2012)

Fig. 2.21 made clear that split tensile strength was maximum for the mix M2 followed by M3, M4, M1 and M5. The increase in the split tensile strength of SCC specimens was due to the better filling effect of the fine particles of QDP in the micro voids of concrete. Thus the data signified that filling ability of 8-10% QDP was better than FA or SF plus QDP.

Boga and Topcu (2012) investigated the influence of fly ash on corrosion resistance and chloride ion permeability of concrete. In this study, fly ash with varying percentages like 0%, 15%, 30% and 45% was used in replacement to CEM 1 42.5R cement to evaluate the split tensile strength of concrete. The samples were tested for 28 and 56 days in two different conditions i.e air and water. Splitting tensile strength was evaluated on cylindrical specimens of diameter100mm and 200mm length.

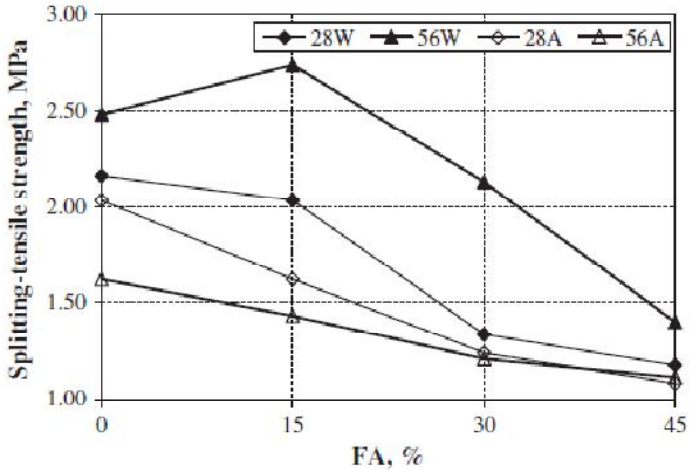

Fig. 2.22 The Variation in Concrete Splitting Tensile Strengths with respect to Fly Ash Ratio (Boga and Topcu, 2012)

It was clearly shown in fig. 2.22 that the highest values were obtained from 56W series in which 15% replacement of cement with FA considered. In W cure conditions, the values of splitting strength were higher than A cure conditions. These increases were 14.71%, 34.38%, 59.52% and 18.92%, respectively according to the use of FA at 0%, 15%, 30% and 45% ratios replace by cement. The decrease in cure A conditions was due to the increase in cure duration. Split tensile strength decreased on the use of FA at 30% and 45% ratios.

Topcu and Canbaz (2007) studied the effect of different fibers on the mechanical properties of concrete containing fly ash. In this test, the cement was replaced by weight with 10%, 15% and 20% of fly ash and effects of addition of steel and polypropylene fibers were experimentally investigated. Use of fly ash provides economical advantages to the production of concrete. The fibers used in concrete

provide better performance whereas, on the other hand fly ash adjusted the workability and strength losses caused by fibers, and improve strength gain. The cement used in the experiment was ASTM Type 1 Portland cement. The fly ash used was Class F type fly ash and fibers with both ends twisted which belong to C type were used.

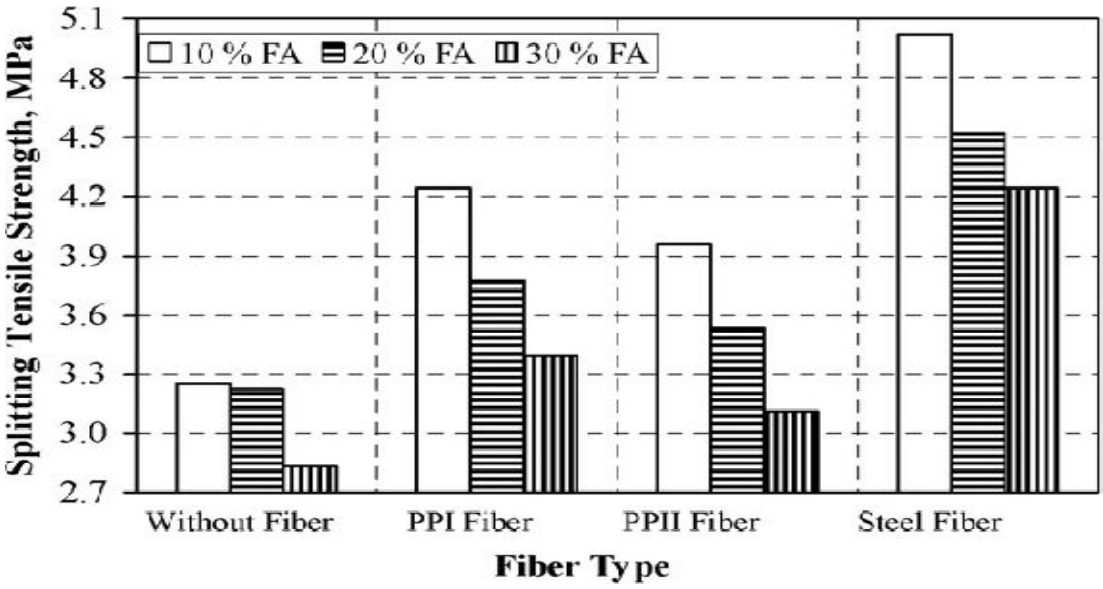

Fig.2.23 The Change of Splitting Tensile Strength versus Fiber Type (Topcu and Canbaz, 2007)

From the results, it made clear that there was significant increase in splitting tensile strength of concrete specimens containing SF fibers. Fibers especially SF fibers make the concrete less brittle and more ductile. Tensile strength of ductile materials is higher than brittle materials.

Table 2.8 Relative Strength of Concrete (Topcu and Canbaz, 2007)

Series	Relative splitting tensile strength (28 days)
A1	100
A2	130
A3	122
A4	154
B1	99
B2	116
B3	109
B4	139
C1	87
C2	104
C3	96
C4	130

Siddique (2003) studied the effect of fine aggregate replacement with Class F fly ash on the mechanical properties of concrete. Fine aggregates were replaced by Class F fly ash with five percentages as 10%, 20%, 30%, 40% and 50%) by weight. Split tensile strength was determined at 7, 14, 28, 56, 91and 365 days.

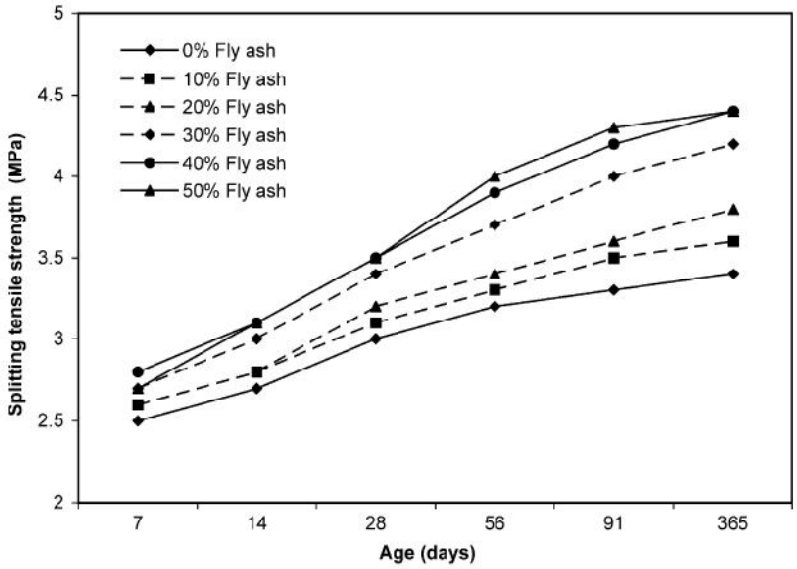

Fig. 2.24 Splitting Tensile Strength versus Age (Siddique, 2003)

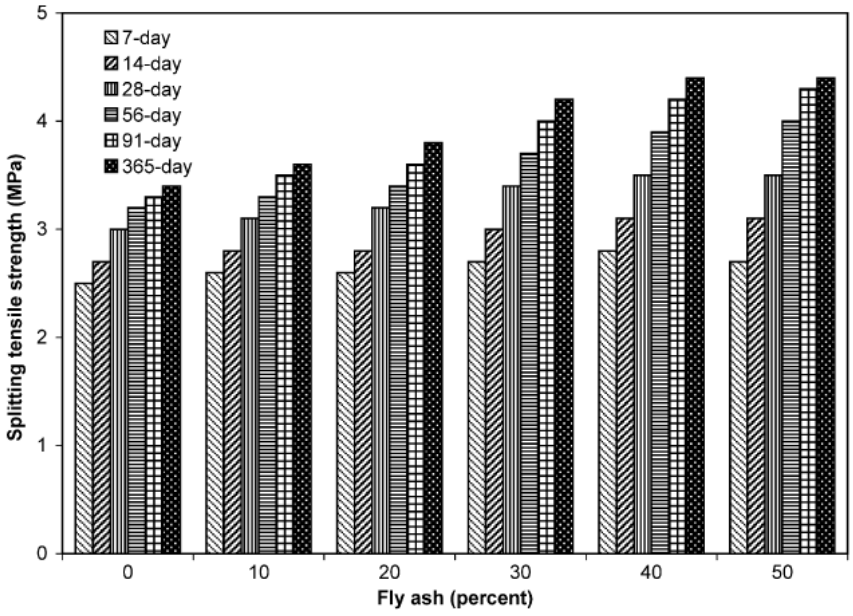

Fig. 2.25 Splitting Tensile Strength versus Fly Ash Percentage (Siddique, 2003)

It was evident that split tensile strength of all mixes continued to increase with the age. Fig. 2.24, fig. 2.25 made clear that there was increase in strength with the increase in fly ash percentages; however, the rate of increase of strength is becoming lesser with the increase in fly ash content. This trend is more obvious between 40% and 50% replacement level. However, maximum strength at all ages occurs at 50%

fine aggregate replacement. The rate of increase in strength is more prominent after 28-days. This may be caused due to the late pozzolanic reaction for forming pozzolanic C–S–H gel between the aggregates and cement fly ash resins.

2.2.3 Young's Modulus

Yoshitake et al. (2013) studied uniaxial tensile strength and tensile Young's modulus of fly-ash concrete at early age. FA used was replaced with cement at replacement ratio of 20%.

Table 2.9 Mix Proportion of Concrete (Yoshitake et al., 2013)

Mix ID	FA0-N	FA20-N	FA20-S	FA20-A	FA20-W
w/b	0.59	0.59	0.59	0.59	0.59
C (kg/m^3)	272	218	218	218	218
W (kg/m^3)	160	160	160	160	160
FA (kg/m^3)	0	54	54	54	54
S1 (kg/m^3)	274	271	271	271	271
S2 (kg/m^3)	274	271	271	271	271
S3 (kg/m^3)	365	362	362	362	362
G1 (kg/m^3)	590	586	586	586	586
G2 (kg/m^3)	394	390	390	390	390
WRA (kg/m^3)	2.72	2.72	2.72	1.36	1.36
AEA (kg/m^3)	0	0.27	0.27	0.41	0.41
Air	3.5%	-	4.4%	4.5%	5.3%
Slump	7.5cm	11.5cm	4.0cm	11.5cm	13.6cm

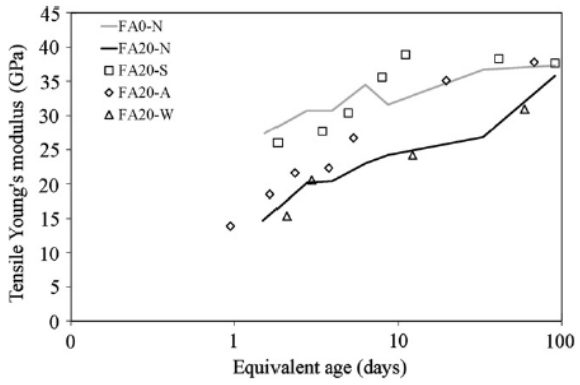

Fig. 2.26 Tensile Young's Modulus-Equivalent Age (Yoshitake et al., 2013)

Fig. 2.26 shows the modulus develops with increasing equivalent age. The modulus of fly-ash concrete cured in the field was equal to or greater than the modulus of fly-ash concrete (FA20-N) made in the laboratory. The different moduli may be caused by the definition of the equivalent age and/or drying condition of each prismatic specimen.

Abu Al-Rub et al. (2012) studied on the aspect ratio effect of multi-walled carbon nanotubes reinforcements on the mechanical properties of cementitious nanocomposites. This study focussed on the effect of different concentrations of long multi-walled carbon nanotubes with high aspect ratios lies in the range of 1250-3750 and short multi-walled carbon nanotubes with aspect ratio of 157 in cement paste. The specimens were tested after 7, 14 and 28 days. Three different batches of MWCNTs i.e. long 0.1% MWCNT, short 0.1% MWCNT, short 0.04% MWCNT, long 0.04% MWCNT, short 0.2% MWCNT were used.

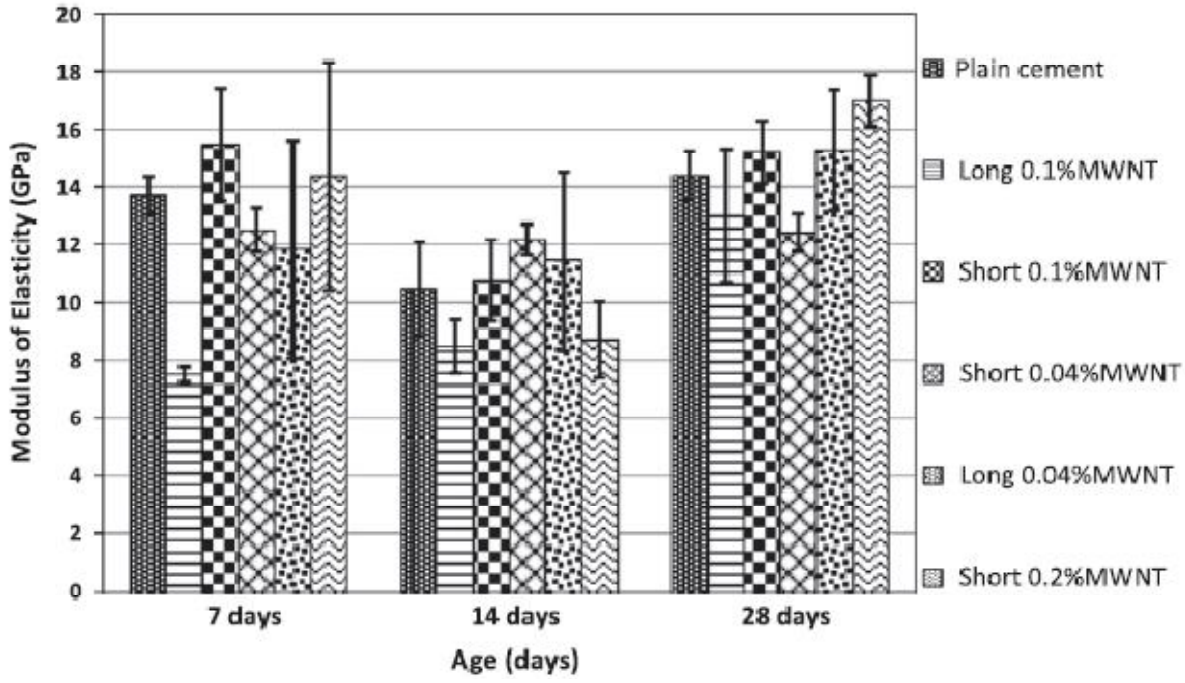

Fig. 2.27Average Modulus of Elasticity for Different MWCNTs Composite Specimens with the Standard Error of the Mean (Abu Al-Rub et al., 2012)

From fig. 2.27, it made clear that the young's modulus decreases from 7 day curing to 14 day curing and then increased.

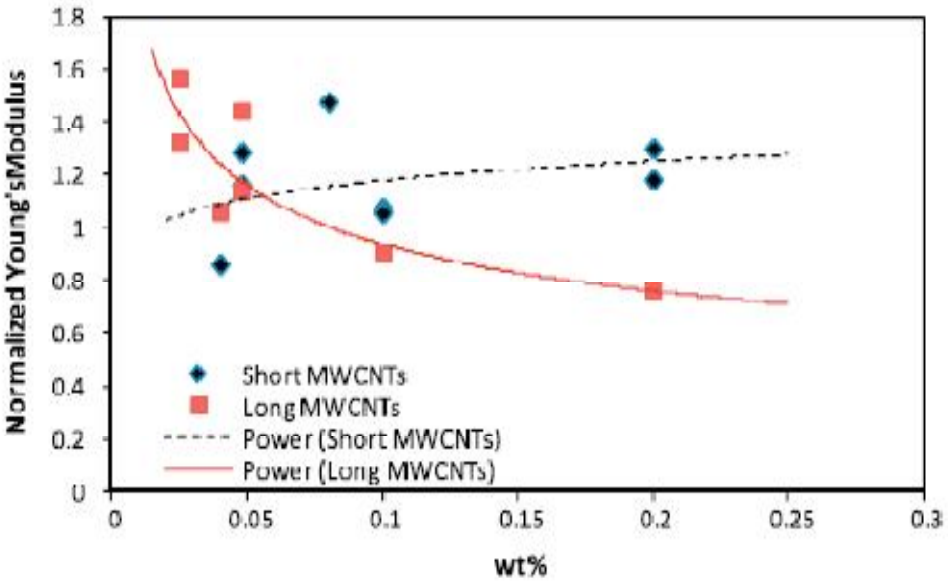

Fig. 2.28 Variation of the Normalized Young's Modulus with the CNTs Concentration for two Different Aspect Ratios; Long and Short (Abu Al-Rub et al., 2012)

It is clearly seen from Fig. 2.28 that the Young's modulus increases as the long-CNTs concentration decreases, whereas the Young's modulus increases as the short-CNTs concentration increases. It is also noticeable that low concentrations of long-CNTs can lead to a much higher increase in the Young's modulus as compared to higher concentrations of short-CNTs. The cause for decrease in young's modulus is clear from the fact that long- CNTs were difficult to disperse as compared to short CNTs. Therefore, to make use of long -CNTs in the matrix, it is desirable to achieve better dispersion since it is expected to lead to a much higher increase in the mechanical properties due to higher SA/V ratio. These results show that the aspect ratio of CNTs plays an important role in the reinforcement of cementitious materials.

Table 2.10 Summary of Obtained Young's Modulus Values from the Literature for CNT/Cement Composites (Abu Al-Rub et al., 2012)

CNTs:% weight of cement	Nanocomposite Young's modulus (MPa)	Control Young's modulus (MPa)	Water/cement ratio	Aspect ratio
Short CNTs				
0.048	19.4	16.7	0.3	300
0.048	11.3	8.8	0.5	300
0.08	13	8.8	0.5	300
0.1	15.9	14.8	0.4	150
0.2	19.2	14.8	0.4	150
0.04	12.4	14.38	0.4	150
0.1	15.2	14.38	0.4	150
0.2	16.98	14.38	0.4	150
Long CNTs				
0.025	22	16.7	0.3	1600
0.048	19	16.7	0.3	1600
0.025	13.8	8.8	0.5	1600
0.048	12.7	8.8	0.5	1600
0.2	17.5	23	0.4	2500
0.04	15.25	14.38	0.4	2500
0.1	12.99	14.38	0.4	2500

Karahan and Atis (2011) investigated the durability properties of polypropylene fiber reinforced fly ash concrete. Fly ash content used in the mix was 0%, 15%, and 30% in mass basis and fiber volume fraction was 0%, 0.05%, 0.10% and 0.20% in volume basis. A polycarboxylic ether based plasticizer i.e. 1% of the cement content was used.

Table 2.11 Mix Proportion (Karahan and Atis, 2011)

Mixture	PC (kg/m^3)	Fly ash (kg/m^3)	PP fiber (kg/m^3)	W (lt/m^3)	HP (kg/m^3)	Aggr. (kg/m^3)
A1	400	-	-	140	4.0	1891
A2	400	-	0.45	140	4.0	1890
A3	400	-	0.90	140	4.0	1889
A4	400	-	1.80	140	4.0	1886
B1	340	60	-	140	4.0	1874
B2	340	60	0.45	140	4.0	1872
B3	340	60	0.90	140	4.0	1871
B4	340	60	1.80	140	4.0	1868
C1	280	120	-	140	4.0	1856
C2	280	120	0.45	140	4.0	1855
C3	280	120	0.90	140	4.0	1853
C4	280	120	1.80	140	4.0	1851

Table 2.12 Young's Modulus Test Results (Karahan and Atis, 2011)

S.no.	Young's mudulus (GPa)	S.no.	Young's mudulus (GPa)	S.no.	Young's mudulus (GPa)
A1	37.9	B1	37.5	C1	36.8
A2	39.0	B2	39.4	C2	37.1
A3	37.2	B3	37.4	C3	34.2
A4	36.7	B4	37.2	C4	35.3

Modulus of elasticity which is also called as secant modulus is taken as slope of the chord from the origin to some arbitrary point on stress-strain curve. The secant modulus calculated in this study is for 40% of the maximum stress. The elasticity modulus of the concrete containing 15% and 30% fly ash were comparable with the elasticity modulus of control Portland cement concrete at 28 days. Elastic modulus of concrete containing 0.05% polypropylene is slightly higher than the elastic modulus of concrete without fibers, whereas with the addition of 0.10% and 0.20% polypropylene fibers, reduce the modulus of elasticity.

Siddique (2003) studied the effect of fine aggregate replacement with Class F fly ash on the mechanical properties of concrete. Fine aggregates were replaced by Class F fly ash with five percentages as 10%, 20%, 30%, 40% and 50%) by weight. Modulus of elasticity was determined at 7, 14, 28, 56, 91and 365 days.

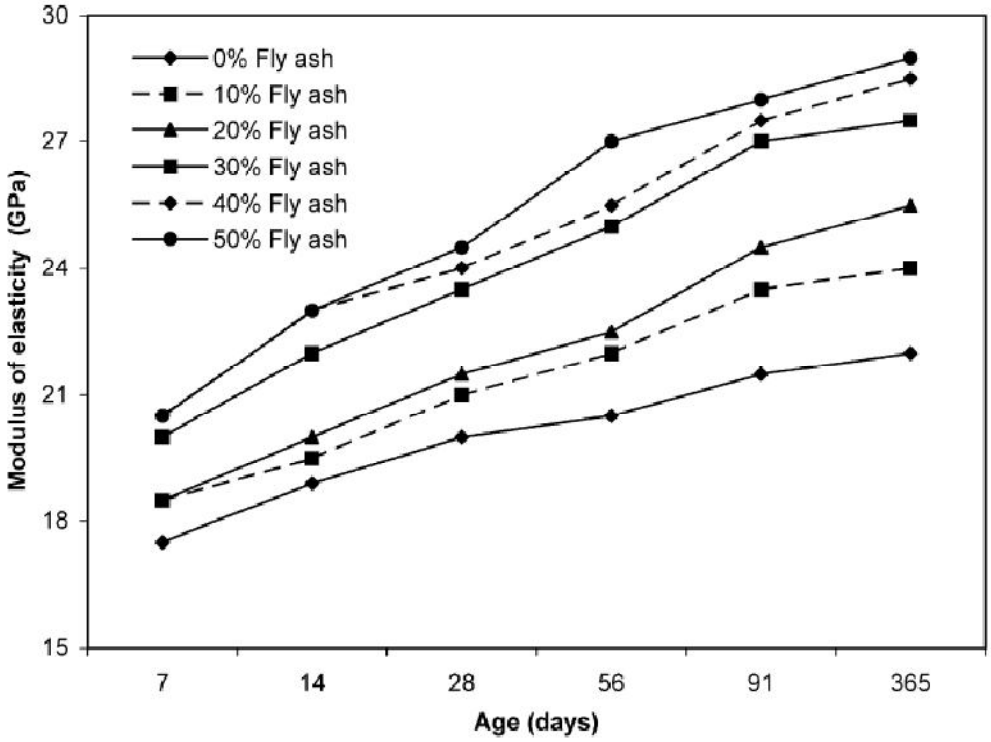

Fig. 2.29 Modulus of Elasticity versus Age (Siddique, 2003)

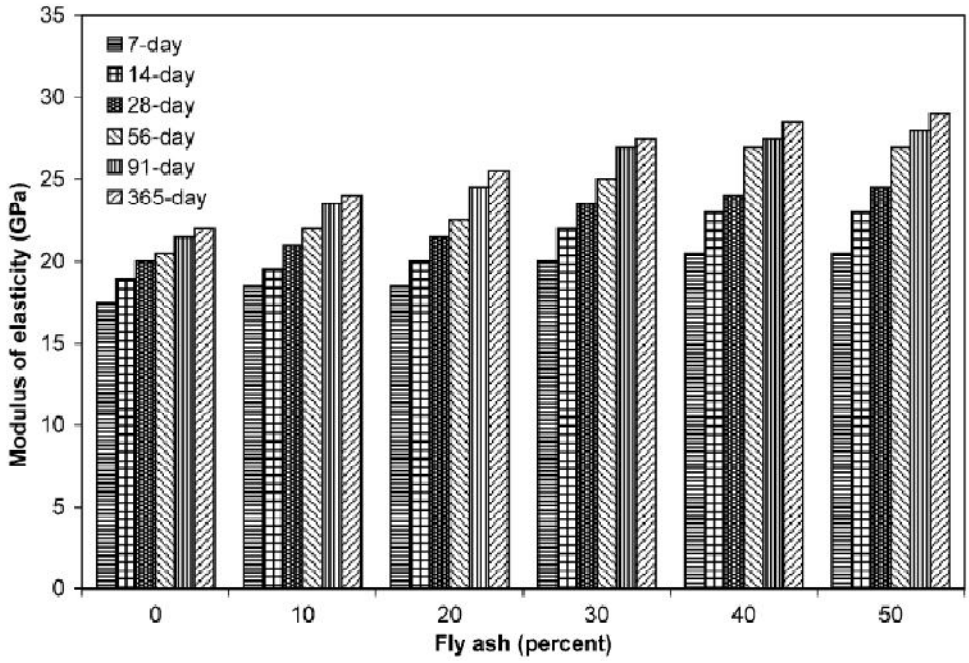

Fig. 2.30 Modulus of Elasticity versus Fly Ash Percentage (Siddique, 2003)

From the test results, it can be seen that the modulus of elasticity of fly ash concretes with 10%, 20%, 30%, 40% and 50% fine aggregate replacement was higher than the control mix at all ages. From fig.2.30, the trend showing that there is increase in young's modulus with increasing percentages of FA. But this was more obvious between 40% and 50% replacement level. The maximum strength occurred at 50% replacement level at all ages.

Bouzoubaa et al. (2001) studied the Mechanical properties and durability of concrete made with high-volume fly ash blended cements using a coarse fly ash. For the easy dispersion of cement blends, a sulphonated naphthalene-formaldehyde condensate type of superplasticizer in a powder form was used.

Table 2.13 Modulus of Elasticity Test Results (Bouzoubaa et al., 2001)

S.no.	W/(C+FA)	Cement type	Young's modulus of Elasticity, GPa	
			28 days	91 days
1	0.32	LPC	22.4	30.6
2	0.32	BCG	34.4	38.7
3	0.40	LPC	30.3	31.6
4	0.42	III	33.0	32.5

The lower E value of Batch 1 was mainly due to its higher air content and low strength.

2.2.4 Rapid Chloride Permeability Test

Nassar et al. (2013) studied field investigation of high-volume fly ash pavement concrete. For performing this test, cores were drilled from pavement and were tested after 270 days of concrete age. High volume fly ash was adopted as a partial replacement in pavement so as to produce durable infrastructure and above all to have an economic concrete pavements. Type 1 Portland cement and Class C fly ash was used for the test. Two types of concrete mix designs were prepared. In control mix, 25% replacement of cement with class C fly ash was made, whereas in HVFA mix 50% replacement was made.

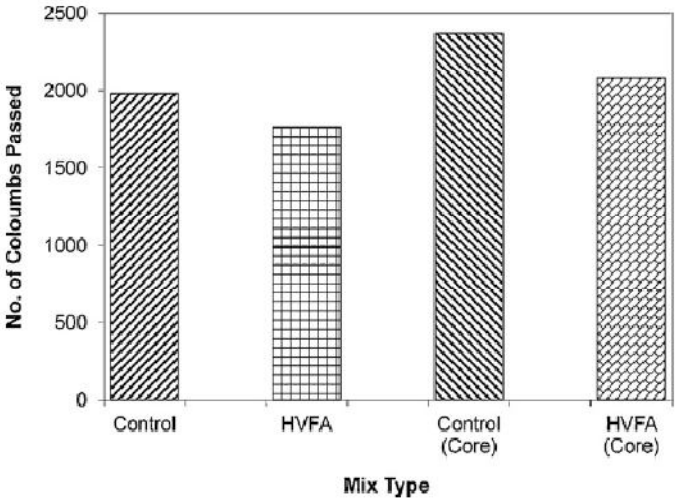

Fig. 2.31 Chloride Permeability Test Results of Field and Core Concrete Specimens (Nassar et al., 2013)

Resistance of concrete to chloride ion penetration gives an indication of the barrier qualities of concrete against salt solution and other aggressive liquids, which critically persuade its long-term durability. Fig. 2.31 demonstrated that the charge passed in control specimens was more as compared to the HVFA concrete. In HVFA concrete, due to the finer sized FA particles, they acted as filler element in the concrete and thus provides barrier for allowing chloride ions to pass through the specimen.

Boga and Topcu (2012) investigated the influence of fly ash on corrosion resistance and chloride ion permeability of concrete. In this study, fly ash with varying percentages like 0%, 15%, 30% and 45% was used in replacement to CEM 1 42.5R cement to evaluate the compressive strength of concrete. The samples were tested for 28 and 56 days in two different conditions i.e air and water. 150x150x150 mm cube specimens were prepared for investigating compressive strength. According to ASTM 1202, the limiting values are listed in table below.

Table 2.14 ASTM 1202 Limit Values (Boga and Topcu, 2012)

Charge passed (Coulombs)	Chloride permeability
>4000	High
2000-4000	Moderate
1000-2000	Low
100-1000	Very low
<100	Negligible

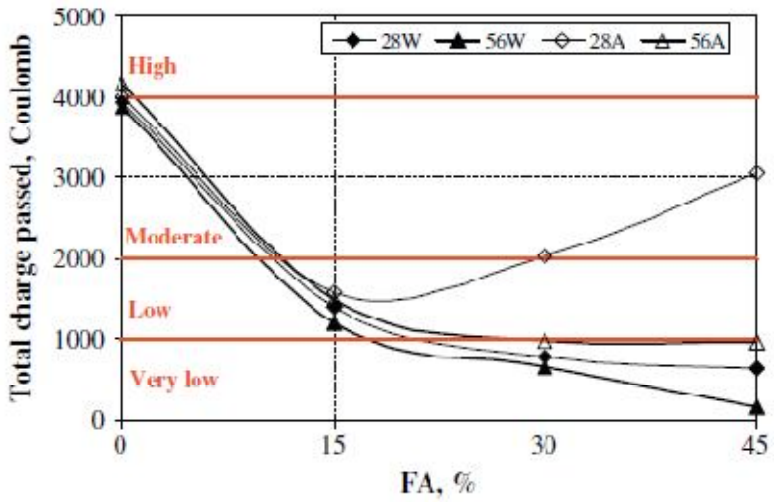

Fig.2.32 Change in Total Charge Passed with Respect to Fly Ash Ratio (Boga and Topcu, 2012)

Through an investigation of Fig.2.32, it was seen that chloride permeability of all series without FA addition are high. It was found that chloride permeability of all series is low when FA is used at 15% ratio replace by cement. It was found that chloride permeability of 28W and 56W series are very low when FA is used at 30% and 45% ratios replaced by cement. When FA was used at 30% and 45% ratios, chloride permeability of 28A series rose to moderate level compared to series at which FA was used 15% ratios. At early stages with higher percentage of FA present in concrete, the pozzolanic reactions could not occur completely, so as a result they lead to higher impermeability of concrete. One reason for the low impermeability of concretes including fly ash is that concretes with fly ash have higher electrical resistances. Other materials like GGBS, silica fume, due to their finer sized property, they got keen interest in chloride permeability. These materials help to bind chloride ions.

Nath and Sarker (2011) studied the effect of fly ash on the durability properties of high strength concrete. Fly ash was used in replacement at 30% and 40% of total binder. The concrete specimens were tested after 28 days and 180 days. The mixture series A was designed with varying water binder ratios whereas mixture B was designed with constant water binder ratio. Concrete cylinders with dia. 100mm and height 200mm were casted.

Table 2.15 Concrete Mix Proportion (Nath and Sarker, 2011)

Series	Mix ID	Binder		Superplasticiser (kg/m^3)	w/b	Slump (mm)
		FA (%)	Cement (kg/m^3)			
A	A-00	0	355	5.11	0.41	140
	A-30	30	308	4.77	0.32	170
	A-40	40	264	4.75	0.31	185
B	B-00	0	517	6.77	0.29	150
	B-30	30	362	4.80	0.29	175
	B-40	40	311	4.24	0.29	160

Table 2.16 Rapid Chloride Permeability Test Results (Nath and Sarker, 2011)

Mix ID	Chloride permeability (Coulomb)	
	28 days	180 days
A-00	2722.0	1652.5
A-30	1757.5	573.0
A-40	1493.0	489.0
B-00	2070.5	910.0
B-30	1881.0	466.0
B-40	1574.0	566.5

Penetrability of Cl- reduced with the increase of fly ash in the mixtures. At 180 days, the Cl^- penetration level decreased to 'Very Low' for the fly ash concretes. The Cl^- penetration values of the fly ash concretes are less than those of the corresponding control concretes at this age. The fly ash concretes in Series A resulted in 35% to 45% reduced Cl^- permeability to that of control concrete at 28 days which further reduced as 65% to 70% in 180 days. Resistance to chloride penetration increased with the increase in fly ash content from 30% to 40% of total binder. On the other hand, for concretes of Series B, inclusion of fly ash reduced Cl^- permeability up to 24% at 28 days which further reduced up to 48% at 180 days. The concrete with 40% fly ash has

shown slightly higher Cl^- penetrability than that with 30% fly ash at 180 days. However, they both were in the range of 'very low' value of charge passed.

Bouzoubaa et al. (2001) studied the Mechanical properties and durability of concrete made with high-volume fly ash blended cements using a coarse fly ash. For the easy dispersion of cement blends, a sulphonated naphthalene-formaldehyde condensate type of superplasticizer in a powder form was used.

Table 2.17 Resistance to Chloride-Ion Penetration (Bouzoubaa et al., 2001)

S.no.	W/(C+FA)	Cement type	Total charge passed, coulombs		
			28 days	91 days	365 days
1	0.32	LPC	1170	320	110
2	0.32	BCG	333	290	105
3	0.40	LPC	2580	2140	n.a
4	0.42	III	2432	2100	n.a

At 91 days, the total charge passed, in coulombs (C), was less than 400 C for the HVFA concretes compared with > 2000 C for the control concrete. The concrete made with the blended cement BCG (Mixture 2) showed higher resistance to the chloride-ion penetration at 28 days than the mixture in which fly ash had been added as a separate ingredient at the concrete mixer. However, at 91 days, the resistance of these two HVFA concrete mixtures was similar.

2.3 SUMMARY

Literature on the utilization of carbon nanotubes plus fly ash is not extensive. Only few studies have been reported on their use to evaluate mechanical as well as durability properties. Therefore, the present study put some contribution to the literature for the same.

CHAPTER 3
EXPERIMENTAL PROGRAM

3.1 GENERAL

The aim of the experimental program is to compare the properties of concrete made with fly ash and varying percentages of CNTs incorporated in concrete. The basic tests carried out on concrete samples are discussed in this chapter, followed by a brief description about mix design and curing procedure adopted. At the end, the various tests conducted on the specimens are discussed.

3.2 MATERIALS

For the entire experimental program, following materials were used.

3.2.1 Cement

Ordinary Portland Cement (OPC) grade 43 (Shree Ultra Tech) was used and tested confirming IS: 8112-1989. Test results were given in table 3.1.

Table 3.1 Physical Properties of Ordinary Portland Cement

Physical Properties	Values obtained	Values as per IS: 8112-1989
Setting time (minutes)		
Initial	95 minutes	Not less than 30 minutes
Final	185 minutes	Not greater than 600 minutes
Compressive strength (MPa)		
3 days	25.03	23
7 days	38.51	33
28 days	45.4	43
Standard consistency (%)	29%	-
Specific gravity	3.12	-

3.2.2 Fine Aggregates

Locally available natural sand with 4.75mm maximum size was used as fine aggregate. The physical properties and sieve analysis are given in Tables 3.2 and Table 3.3 respectively.

Table 3.2 Physical Properties of Fine Aggregates

S.no.	Characteristics	Value
1.	Type	Natural sand
2.	Specific Gravity	2.64
3.	Fineness Modulus	2.55
4.	Grading Zone	III

Table 3.3 Sieve Analysis of Fine Aggregates

S.no.	Sieve size	Weight retained (Grams)	Percentage retained (%)	Percentage Passing (%)	Cumulative percentage retained (%)
1.	4.75 mm	5	0.50	99.50	0.50
2.	2.36 mm	59	5.90	93.60	6.40
3.	1.18 mm	136	13.60	80.00	20.00
4.	600 mm	243	24.30	55.70	44.30
5.	300 mm	415	41.50	14.20	85.80
6.	150 mm	122	12.20	2.00	98.00
7.	Pan	20	2.00	-	-
					ΣF = 255

Fineness modulus = ΣF/100= 2.55

3.2.3 Coarse Aggregates

Crushed stone with maximum 20mm graded aggregates were used. Physical properties and sieve analysis results are given in Tables 3.4 and Table 3.5 respectively.

Table 3.4 Physical Properties of Coarse Aggregates

Properties	Observed values
Maximum size (mm)	20
Specific gravity	
10mm	2.667
20mm	2.701
Total water absorption (%)	1.8
Fineness modulus	7.68

Table 3.5 Sieve Analysis of Coarse Aggregates

S.no.	Sieve size	Weight retained (kg)	% retained	% passing	Cumulative % weight retained
1.	20 mm	0	0	100	0
2.	12.5 mm	2.1865	72.883	27.117	72.833
3.	10 mm	0.6745	22.483	4.634	95.366
4.	4.75 mm	0.1390	4.633	0.01	99.99
					∑C= 268.18

Fineness Modulus = (∑C+500)/100 = 7.68

3.2.4 Fly Ash

Class F Fly ash produced from "Thermal Power Station, Bathinda" Punjab was used.

3.2.5 Carbon Nanotubes

Carbon nanotubes used in the experiment were synthetic graphite (multiwalled carbon nanotubes) with max. 5% inorganic impurity. The manufacturer/supplier of carbon nanotubes was Plasma Chem GmbH, Berlin Rudower Ch. 29, D-12489. For the experiment, CNTs were ordered from Reinste Nano Ventures Pvt. Ltd., New Delhi.

Table 3.6 Physical Properties of CNTs

Physical property	Observed Values
Form	Powder
Colour	Black
Carbon purity	Min. 95%
Number of Walls	3-15
Outer diameter	5-20nm
Inner diameter	2-6nm
Length	1-10μm
Apparent density	0.15-0.35g/cm^3
Loose agglomerate size	0.1-3mm
Flash point	>290℃
Danger of explosion	At concentrations 50g/m^3 and higher
Density at 20℃	0,15 g/cm^3
Water	Insoluble

3.2.6 Water

Generally, water that is suitable for drinking is satisfactory for use in concrete. Water from lakes and streams that contain marine life also usually is suitable. When water is obtained from sources mentioned above, no sampling is necessary. When it is supposed that water may contain sewage, mine water, or wastes from industrial plants or canneries, it should not be used in concrete unless tests indicate that it is satisfactory. In the present experimental programme, potable tap water is used for casting.

3.3 DISPERSION OF CNTs

3.3.1 Ultrasonicator Bath

As CNTs are insoluble in water, so to make their use as an additive in concrete, they should dispersed in water by making use of ultrasonicator bath. CNTs got dispersed in water after sonication in the bath tubs for 1 hour. In liquid, the rapid vibration of the tip causes cavitation, the formation and violent collapse of microscopic bubbles. The collapse of thousands of cavitation bubbles releases tremendous energy in the cavitation field. Objects and surfaces within the cavitation field are “processed.” By

increasing the amplitude setting, cavitation intensity within the sample is also increased.

3.4 METHODOLOGY ADOPTED FOR MIX DESIGN

Mix design is a process of selecting suitable ingredients for concrete and determining their proportions which would produce economical concrete. The proportioning of the ingredients of concrete is an important segment of concrete technology as it ensures quality and economy. For obtaining the concrete of desired performance characteristics, the component materials should be selected likewise. Then by considering these components, appropriate mix design is prepared.

3.4.1 Design of Concrete Mix

The compressive strength is said to be the index of quality of concrete. Therefore the design mix should be prepared keeping in view compressive strength of concrete with adequate workability so that the fresh concrete can be properly mixed, placed and compacted. The proportions for the mix were calculated adopting the requirements of water as specified in IS: 10262-2009.

The following three steps must be followed for proportioning of concrete mixes.

(i) Selection of suitable ingredients-cement, supplementary cementing materials, aggregates, and water and chemical admixtures (if required).

(ii) Determination of the relative quantities of components to have economical concrete, that has desired rheological properties i.e. strength and durability.

(iii) Careful quality control of every phase of the concrete making process.

In the present study Mix Design (Design value at the age of 28 days) grade concrete is done according to BIS: 10262-2009

Design mix

Degree of quality control expected at site	=	Good
Max. Size of aggregate used	=	20mm
Water/cement	=	0.5
Fly ash	=	20% by weight of cement

Ingredients of concrete are listed in table 3.7

Table 3.7 Mix Proportion

Unit of batch	Cement (kg)	Fine aggregates (kg)	Coarse aggregates (kg)		Water (litres)
			10mm	20mm	
Cubic meter content	364	593.58	600.33	588.67	182
Ratio of Ingredients	1	1.631	1.65	1.617	0.5

3.4.2 Mix Composition

The concrete mixes were prepared with constant quantities of fine, coarse aggregates and water. Five types of mixes were prepared. Their description is shown in table 3.8. Fly ash (FA) was introduced in concrete on replacement with cement (20%) by weight. Also CNTs were incorporated in addition to concrete with varying percentages as 0.025%, 0.048%, and 0.08% by weight of (Cement + Fly ash) mixture.

Table 3.8 Detailed Descriptions of Concrete Mixes

Mix	FA (Replacement by weight of cement) (%)	CNT (Addition to concrete (cement+fly ash) by weight) (%)
Control Mix (CM)	0	0
FA20	20	0
FA20-C0.025	20	0.025
FA20-C0.048	20	0.048
FA20-C0.08	20	0.08

Table 3.9 Concrete Mixes

Mix	CM	FA20	FA20-C0.025	FA20-C0.048	FA20-C0.08
Cement (kg/m^3)	364	291.2	291.2	291.2	291.2
Fine aggregates (kg/m^3)	594	594	594	594	594
Coarse aggregates (kg/m^3)	1189	1189	1189	1189	1189
Replacement FA (%)	-	20%	20%	20%	20%
Fly ash (kg/m^3)	-	72.8	72.8	72.8	72.8
Water/cement	0.5	0.5	0.5	0.5	0.5
Water (litres)	182	182	182	182	182
CNT (%)	-	-	0.025%	0.048%	0.08%
CNT (kg/m^3)	-	-	9.1	17.47	29.12

3.5 CASTING OF SPECIMENS

All the specimens were casted referring to the mix proportions mentioned in table 3.9 and table 3.10. For these mix proportions, required quantities were weighed. Under this article, casting of specimens for different properties is mentioned.

3.5.1 Specimens for Compressive Strength

150x150x150 mm sized cube specimens were prepared for compressive strength. The materials required were weighed according to the mix proportion. Cement, fly ash, fine aggregates and coarse aggregates were dry mixed first to have a uniform colour. After that 50% of the total water required was added to the mix to have thorough mixing for 3-4 minutes. Then 40% of the water was added with addition of sonicated CNTs to the mix. Remaining 10% of water was sprinkled on the above mix and it was thoroughly mixed in the mixer. The oiled samples were then filled with the mix prepared and then filled moulds were put on the vibrating table for their proper mixing. Immediately after casting cubes, the specimens were covered with gunny bags to prevent water evaporation. Six identical cubes were casted. Out of six, three were tested after 7 days and rest after 28 days of curing.

3.5.2 Specimens for Split Tensile Strength

150x150x150 mm sized cube specimens were prepared for split tensile strength. The materials required were weighed according to the mix proportion. Cement, fly ash, fine aggregates and coarse aggregates were dry mixed first to have a uniform colour. After that 50% of the total water required was added to the mix to have thorough mixing for 3-4 minutes. Then 40% of the water was added with addition of sonicated CNTs to the mix. Remaining 10% of water was sprinkled on the above mix and it was thoroughly mixed in the mixer. The oiled samples were then filled with the mix prepared and then filled moulds were put on the vibrating table for their proper mixing. Immediately after casting cubes, the specimens were covered with gunny bags to prevent water evaporation. Six identical cubes were casted. Out of six, three were tested after 7 days and rest after 28 days of curing.

3.5.3 Specimens for Young's Modulus

Diameter 150mm and 300mm length sized cylinder were casted for young's modulus. The materials required were weighed according to the mix proportion. Cement, fly ash, fine aggregates and coarse aggregates were dry mixed first to have a uniform colour. After that 50% of the total water required was added to the mix to have thorough mixing for 3-4 minutes. Then 40% of the water was added with addition of sonicated CNTs to the mix. Remaining 10% of water was sprinkled on the above mix and it was thoroughly mixed in the mixer. The oiled samples were then filled with the mix prepared and then filled moulds were put on the vibrating table for their proper mixing. Immediately after casting cylinders, the specimens were covered with gunny bags to prevent water evaporation. Six identical cylinders were casted. Out of six, three were tested after 7 days and rest after 28 days of curing.

3.5.4 Specimens for Rapid Chloride Permeability

The resistance to chloride penetration of concrete was determined by casting cylinders of size diameter 100mm and length 200mm. The materials required were weighed according to the mix proportion. Cement, fly ash, fine aggregates and coarse aggregates were dry mixed first to have a uniform colour. After that 50% of the total water required was added to the mix to have thorough mixing for 3-4 minutes. Then 40% of the water was added with addition of sonicated CNTs to the mix. Remaining 10% of water was sprinkled on the above mix and it was thoroughly mixed in the mixer. The oiled samples were then filled with the mix prepared and then filled moulds were put on the vibrating table for their proper mixing. Immediately after

casting cylinders, the specimens were covered with gunny bags to prevent water evaporation. Six identical cylinders were casted. Out of six, three were tested after 7 days and rest after 28 days of curing.

3.6 TESTING OF SPECIMENS

After casting, specimens were tested after 7 and 28 days of curing. Under this article, the procedure followed for testing of specimens is mentioned for evaluating various properties like compressive strength, splitting tensile strength, young's modulus of elasticity and rapid chloride permeability of concrete.

3.6.1 Mechanical Properties

3.6.1.1 Compressive Strength

Specimens were demoulded after 24 hours of casting. Then they were poured in curing tank for the predefined time. At the age of testing, specimens were taken out of the tank and allowed surface drying for 10-15 minutes. Specimens were tested in Compression Testing Machine (CTM) at the load rate of 5 kN/sec specified as per IS: 516-1959. CTM has the capacity of 5000kN. The failure load was then evaluated.

Fig. 3.1 Setup for Compressive Strength

3.6.1.2 Split Tensile Strength

Specimens were demoulded after 24 hours of casting. Then they were poured in curing tank for the predefined time. At the age of testing, specimens were taken out of

the tank and allowed surface drying for 10-15 minutes. Specimens were tested in Universal testing machine (UTM) at the load rate of 70 kN/min. UTM has the load capacity of 1000kN. The failure load was then evaluated. The formula used is

$$\text{Split tensile strength} = \frac{0.5187 \times P}{S^2}$$

P = Failure load, in N

S = Side of cube, in mm

Fig. 3.2 Setup for Split Tensile Strength

3.6.1.3 Young's Modulus

The modulus of elasticity or Young's modulus is defined as the slope of the stress strain curve with the proportional limit of a material. Specimens were demoulded after 24 hours of casting. Then they were poured in curing tank for the predefined time. At the age of testing, specimens were taken out of the tank and allowed surface drying for 10-15 minutes. The young's modulus was evaluated using extensiometer in Universal testing machine (UTM). The extensiometer consist of two frames for clamping to the specimens by means of three tightening screws. Two spacers hold the two frames in positions. Dial gauge was already fitted on the extensiometer, which provides deflection. The least count of dial guage was 0.025mm. 3 cycles of loading

was applied on the specimen. Rate of loading was 14N/mm^2/min. The values obtained from first cycle were disregarded and the average of second and third cycle was recorded.

Fig. 3.3 Setup for Young's Modulus using Extensiometer

3.6.2 Durability Properties

3.6.2.1 Rapid Chloride Permeability Test

A durable concrete is the one that performs satisfactorily under anticipated exposure condition during its service life span. One of the main characteristics influencing the durability of concrete is its permeability to the access of chloride. The chloride ion present in the concrete can have harmful affect on concrete as well as on the reinforcement. Swelling of concrete due to chloride ion penetration is 2 to 2.5 times larger than that observed with water penetration. So this test covers the experimental evaluation of electrical conductance of concrete to provide rapid indication of concrete resistance against chloride ion penetration.

The test method (according to ASTM C 1202-97) covered the determination of the electrical conductance of concrete to provide a rapid indication of its resistance to the penetration of chloride ions. According to table 3.10 the chloride ion penetrability was decided on the basis of charge passed. The test method consisted of monitoring the amount of electrical current passed through 2-in. (51-mm) thick slices of 4-in. (102-

mm) nominal diameter cores or cylinders for a 6-h period. A potential difference of 60 V dc was maintained across the ends of the specimen, one of which was immersed in a sodium chloride solution, the other in a sodium hydroxide solution. The total charge passed, in coulombs, was related to the resistance of the specimen to chloride ion penetration.

The cylinders of diameter100mm and 200mm length were casted. Specimens were placed in the vacuum desiccator's bowl as shown in Fig 3.4 which illustrates the setup of the vacuum pump, desiccator with stopcock, vacuum gauge and valve and the deaerated water container after the water has filled the desiccators. The vacuum was maintained in the desiccators bowl for 3 hours. The de-aerated water was allowed to flow into the desiccator, so that it completely covers the specimens and no air was allowed to enter. Again the vacuum was maintained for another one hour. The liquids (3.0% NaCl and 0.3 N NaOH solutions) were filled in the two cells. Power supply was set to 60V, and initial current reading was recorded. Set up of the apparatus is shown in Fig.3.5. Temperatures of the specimen, applied voltage cell and solutions were maintained at 20 to 25℃ at the time the test was initiated (when the power supply was turned on). The values for the charge passed were recorded.

Table 3.10: Chloride Ion Penetrability based on Charge Passed (ASTM 1202-97)

Charge passed (Coulombs)	Chloride ion permeability
>4000	High
2000-4000	Moderate
1000-2000	Low
100-1000	Very low
<100	Negligible